

Article

# Paleoenvironmental Evolution and Organic Matter Accumulation in a Hydrocarbon-Bearing Depression in the East China Sea

Junming Zhan <sup>1</sup> , Entao Liu <sup>1,\*</sup> , Si Chen <sup>2,\*</sup> , Qiyang Zhang <sup>2</sup>, Yuyue Chen <sup>1</sup>, Jialin Zhong <sup>1</sup>, Yongkun Zhou <sup>1</sup>, Peifeng Yang <sup>2</sup> and Yangshuo Jiao <sup>1</sup>

<sup>1</sup> Hubei Key Laboratory of Marine Geological Resources, China University of Geosciences, Wuhan 430074, China

<sup>2</sup> Key Laboratory of Tectonics and Petroleum Resources of Ministry of Education, China University of Geosciences, Wuhan 430074, China

\* Correspondence: liuentao@cug.edu.cn (E.L.); sichen720@hotmail.com (S.C.); Tel./Fax: +86-27-6788-6151 (E.L.); +86-27-6788-3051 (S.C.)

**Abstract:** Investigating the paleoenvironment and characteristics of source rocks in sedimentary basins is crucial for understanding organic matter accumulation and guiding hydrocarbon exploration. The Lishui Sag, a significant hydrocarbon-bearing depression in the East China Sea, has experienced extensive marine transgression and increasing salinity in the Paleocene, but the changes in accumulation factors of organic matter during this evolution process remain unclear. Through a comprehensive analysis of total organic carbon (TOC), major and trace elements, and biomarker data, this study investigates the characteristics of source rocks from two lithostratigraphic units, namely the Paleocene Yueguifeng and Lingfeng formations, to gain deep insight into the effects of paleoenvironment on organic matter accumulation and hydrocarbon distribution. Our results indicate that the Lishui Sag transitioned from a closed lake to an open-marine environment in the Paleocene, with a shift from warm-humid to arid climate conditions. The biomarker distribution suggests a change in the origin of organic matter, with a higher input of terrestrial organic matter in the Lingfeng Formation. During the early stage, the lacustrine source rocks in the lower Yueguifeng Formation were formed in a relatively humid and anoxic environment within brackish water, resulting in a substantial influx of terrestrial and lacustrine algae organic matter. In contrast, in the late stage, the marine source rocks in the overlying Lingfeng Formation were developed in an arid and oxidizing environment. The lacustrine source rocks in the Yueguifeng Formation were notably more favorable to developing good-quality source rocks. Compared with the other regions, the western and northeastern parts of the study area have greater hydrocarbon generation potential due to the wider distribution of high maturity and organic-rich source rocks, with higher terrestrial and algal organic matter input. Moreover, considering the practical circumstances in the exploration, the northeastern part of the Lishui Sag is recommended as the next exploration target zone.

**Keywords:** depositional environment; organic matter accumulation; hydrocarbon exploration; source rocks; East China Sea



**Citation:** Zhan, J.; Liu, E.; Chen, S.; Zhang, Q.; Chen, Y.; Zhong, J.; Zhou, Y.; Yang, P.; Jiao, Y. Paleoenvironmental Evolution and Organic Matter Accumulation in a Hydrocarbon-Bearing Depression in the East China Sea. *J. Mar. Sci. Eng.* **2023**, *11*, 2341. <https://doi.org/10.3390/jmse11122341>

Academic Editor: George Kontakiotis

Received: 7 November 2023

Revised: 8 December 2023

Accepted: 8 December 2023

Published: 12 December 2023



**Copyright:** © 2023 by the authors. Licensee MDPI, Basel, Switzerland. This article is an open access article distributed under the terms and conditions of the Creative Commons Attribution (CC BY) license (<https://creativecommons.org/licenses/by/4.0/>).

## 1. Introduction

The organic matter accumulation rules in sedimentary basins have been the subject of extensive research due to their significant economic potential [1–4]. They are influenced by various factors, including sources of organic material, sedimentation, and preservation. These factors are further associated with the inputs of organic carbon, reducing conditions, and their combined effect [5–7]. Two fundamental conditions govern the formation process of source rocks: the supplement of organic material and its preservation [6,8]. The former highlights the importance of favorable climatic conditions and brackish water as key factors

in generating abundant organic matter [8,9], while the latter underscores the necessity of preserving organic matter in a relatively reducing environment [10,11]. Smith and Bustin (1998) [12] suggested that both a high supply of organic material and effective preservation are critical factors for organic matter accumulation in mudstones. Mayers and Ishiwatari (1993) [13] demonstrated that the structure, morphology, and organic matter enrichment process jointly controlled the abundance of organic matter. Liu et al. (2016) [14] proposed that the medium salinity is more favorable for organic matter accumulation in the Qaidam Basin. However, previous studies on lacustrine organic matter accumulation have primarily focused on either marine or lacustrine depositional settings, and little attention has been paid to the changes in accumulation factors of organic matter during this evolution process from lacustrine to the marine environment [15].

Paleoenvironment changes (e.g., climate, salinity, redox conditions, and terrestrial inputs) have a significant impact on the biological evolution and distribution of organic carbon [1,16,17]. Organic and inorganic geochemical indicators have been widely used to indicate ancient environments. For example, green algae and *Botryococcus braunii* are indicative of a freshwater environment [18,19], while oleananes and retene are commonly developed in terrestrial settings [20]. Abundant diterpenoids (e.g., abietan and retene) are typically derived from gymnosperms, whereas angiosperms produce substantial quantities of triterpenoids (e.g., oleananes, ursanes, and lupanes) [18–20]. Additionally, some indicators are also used for assessing the thermal maturity, carbon content, kerogen types, and depositional environments of source rocks [21–28]. For instance, short-chain *n-alkanes* are predominantly related to aquatic sources (e.g., microphytoplankton), while abundant long-chain *n-alkanes* indicates extensive input of terrestrial organic carbon [29]. The values of Pristane (Pr) and Phytane (Ph) are widely used to indicate redox conditions [30–32].

In the East China Sea, exploration efforts have predominantly centered on the Xihu and Lishui Sags in recent years because of their abundant natural gas and oil resources [33,34]. The previous studies suggest that the Lishui Sag holds the most potential for hydrocarbon exploration [34–37]. However, the paleoenvironmental evolution process and organic matter accumulation rule in the Paleogene remain controversial. The Yueguifeng and Lingfeng formations are confirmed as the main source rocks in the Lishui Sag, characterized by great thickness, deep burial, high organic matter abundance, and high maturity [34–36]. Compared to the overlying Lingfeng Formation, the source rocks in the Yueguifeng Formation are marked by lower Pr/Ph ratios but higher gammacerane concentrations [32–34,38,39], indicating a shift from an anoxic to a relatively oxidizing sedimentary environment. However, the environmental evolution process and the factors governing organic matter accumulation remain unclear. Some studies suggest that the Lishui Sag underwent a transition from a warm-humid to a hot-arid climate, accompanied by fluctuations in salinity [39,40]. Conversely, opposing viewpoints assert that the hot-arid climate transformed into a warm-humid climate during the Paleocene [41]. These environmental factors played a pivotal role in the preservation of organic matter, which in turn impacted the quality, type, and distribution of source rocks [42–44]. The current limitations in these aspects hamper further exploration of oil and gas resources in the Lishui Sag [38].

In this study, we utilized organic and inorganic geochemical parameters to reconstruct the paleoenvironment of lacustrine (Yueguifeng Formation) and marine (Lingfeng Formation) source rocks. We investigate the paleoenvironmental evolution process and the mechanism of organic matter accumulation in the lower and middle Paleocene (66–59.2 Ma). Finally, we conduct a detailed interpretation of the integrated organic characteristics and paleoenvironmental traits of the source rocks, offering valuable proposals for further exploration in the Lishui Sag.

## 2. Geological Setting

The East China Sea shelf basin is a hydrocarbon-bearing backarc rift basin extending in the NNE-SSW direction. It has been influenced by the collisions of the Asian, Pacific, South China Sea, and Philippine plates [34,39,45,46]. The Lishui Sag is a typical Cenozoic rift

basin located in the southwest of the East China Sea shelf Basin. It formed on a Mesozoic basement and is bounded by the Jiaojiang Sag to the north, the Minzhe Uplift to the west, and the Yandang Uplift to the east [47]. It can be subdivided into western and eastern regions, which are separated by the Lingfeng Uplift in the middle (Figure 1).

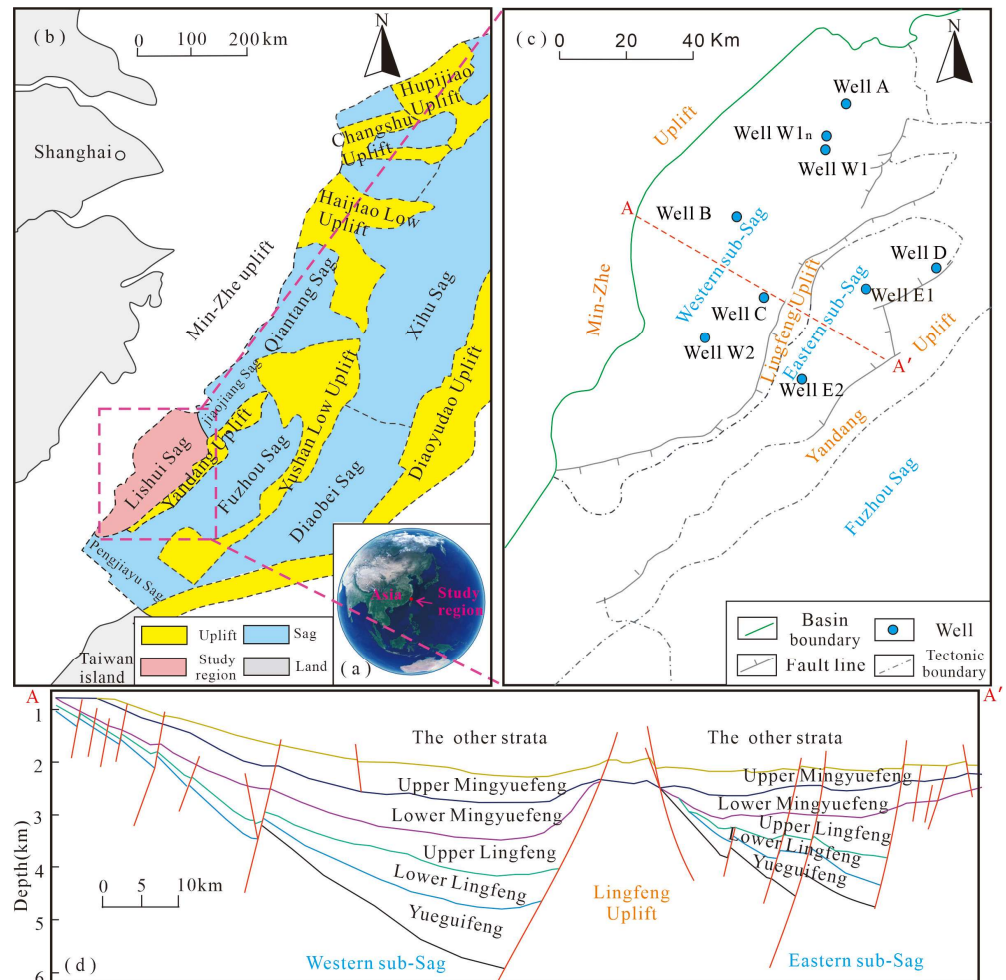


**Figure 1.** Tectonic units of the East China Sea basin and the location of each subsbasin. The Lishui Sag is an important oil prospecting basin located in the southwest of the East China Sea basin. (Modified after Zhong et al., 2018; Xu et al., 2020 [48,49]). (a) Map showing the global location of the study region, (b) geological map showing tectonic units of the East China Sea basin, (c) map showing the tectonic units and tectonic setting of Lishui Sag, (d) interpreted NW-SE trending profile in the Lishui Sag, and the location of the profile is shown in Figure 1c.

The Lishui Sag has undergone a complex tectonic evolution, for which a four-phase model has been proposed: (1) a late Cretaceous to Paleocene period of syn-rift phase, (2) an Eocene period of post-rift phase, (3) a late Eocene to Miocene period of uplifting phase, and (4) a late Miocene to Quaternary period of regional subsidence phase [33]. The Paleocene strata in the Lishui Sag consists of the Yueguifeng Formation (66~61.6 Ma, lower Paleocene), Lingfeng Formation (61.6~59.2 Ma, middle Paleocene), and Mingyuefeng Formation (59.2~56 Ma, upper Paleocene) from bottom to top, respectively (Figures 1d and 2). The Lingfeng Formation and Mingyuefeng Formation can be divided into upper and lower members for each formation. The Yueguifeng Formation and Lingfeng Formation are widely recognized as the main units of hydrocarbon source rocks [39,45,48].

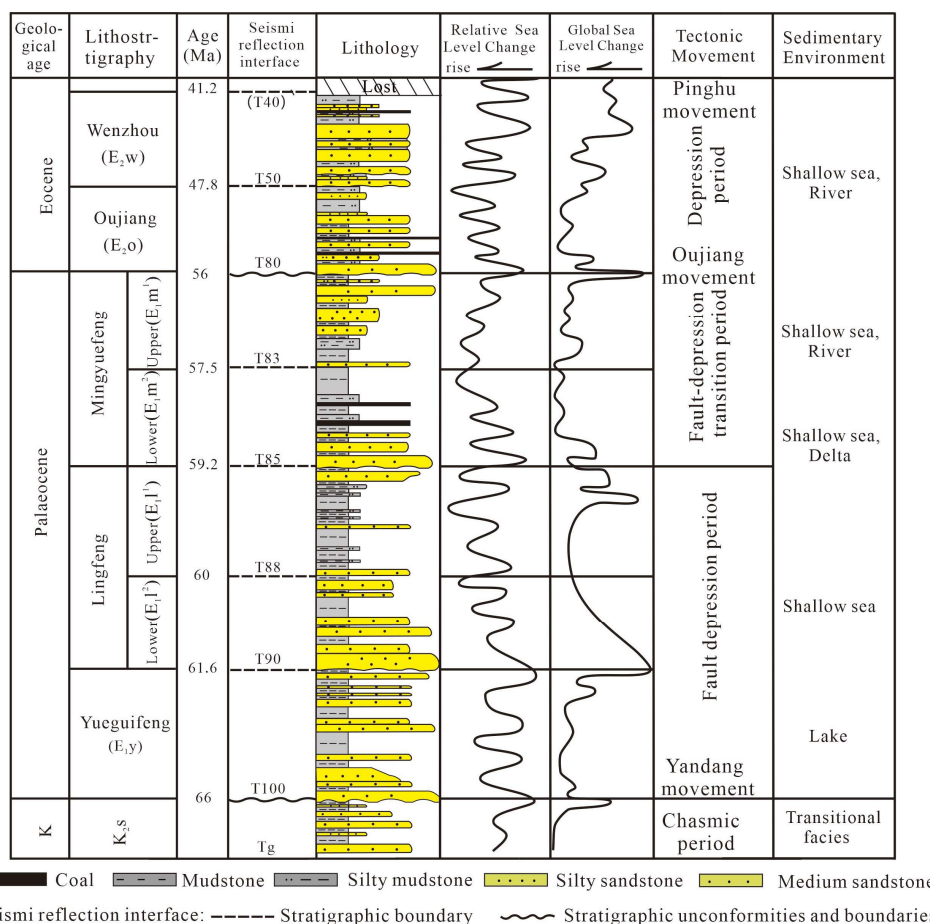


**Figure 2.** Chronostratigraphic chart of the Lishui Sag. From the bottom to top, the Palaeocene stratigraphy includes Yueguifeng, a lower member of the Lingfeng, an upper member of the Lingfeng, a lower member of the Mingyuefeng and an upper member of the Mingyuefeng formations (Modified after Fu et al., 2022 and Miller et al., 2005 [32,50]).

The Yueguifeng Formation is mainly composed of gray lacustrine mudstones and light gray sandstones. The lower member of the Lingfeng Formation is mainly dominated by marine sedimentary rocks with gray muddy sandstones and mudstones, and the upper member of the Lingfeng Formation is mainly marine sedimentary rocks with gray-black mudstones. The Mingyuefeng Formation is mainly composed of gray mudstones and muddy sandstones. In the study area, the sedimentary environment of the lower member of the Lingfeng Formation is in a transition period (62~61 Ma, lower Paleocene) from terrestrial to marine facies. The Lingfeng Uplift partially submerged due to transgression, and the meandering river deltas mainly occurred in the western region. Large-scale fan deltas were mainly developed in the eastern region [47].

### 3. Sample and Experimental Methods

#### 3.1. Samples

All mudstone samples (each sample was about 500 g) of the Yueguifeng and the Lingfeng formations were provided from the Shanghai Branch of China National Offshore Oil Corporation (CNOOC), China. for experiments. All mudstone samples were cleaned, and were then pulverized into 100 or 200 mesh powder for major-trace element experiments (51 samples), total organic carbon (TOC) (135 samples), rock-eval pyrolysis (135 samples), gas chromatography (GC) (25 samples), and gas chromatography-mass spectrometry (GC-MS) (25 samples) analysis. The drilling cores are located far from the offshore (Figure 1c) and the detailed experimental design for the specific samples can be found in Tables S1–S3.

### 3.2. TOC and Rock-Eval Pyrolysis

TOC analysis (each powder sample about 110 mg) was measured in the instrument model CS230 carbon-sulfur determination analyzer. A total of 135 samples were dried and weighed 80–120 mg before the pyrolysis experiments. Then they were placed on the OGE-VI instrument produced by China Petroleum Exploration Institute for automatic TOC analysis.

### 3.3. Major and Trace Elements Analysis

Both major and trace element experiments were conducted at the Wuhan Sample Solution Analytical Technology Co., Ltd., Wuhan, China. The compositions of the main elements were determined by X-ray fluorescence (XRF) of the molten glass disk, and the contents of trace elements in the whole rock were analyzed by Inductively coupled plasma mass spectrometry (ICP-MS). The detailed sample-digesting procedure was described as follows: (1) About 50 mg sample powder was accurately weighed and put into a Teflon bomb after being dried in a 105 °C oven for 12 h; (2) 1 mL HNO<sub>3</sub> and 1 mL HF were slowly added into each Teflon bomb and then they were placed in a stainless steel pressure jacket and heated to 190 °C in an oven more than 24 h; (3) After cooling, they were opened and placed on a hotplate at 140 °C to evaporate incipient dryness, and then they were poured into 1 mL HNO<sub>3</sub> and evaporated to dryness again; (4) 1 mL of HNO<sub>3</sub>, 1 mL of MQ water and 1 mL internal standard solution of In was added, and the Teflon bomb was resealed and placed in the oven at 190 °C over 12 h; (5) The final solution was transferred to a polyethylene bottle and diluted to 100 g by the addition of 2% HNO<sub>3</sub>. The detailed test methods, instruments, and procedures of the major and trace elements can be found in the reference [50].

### 3.4. GC and GC-MS Analysis

A total of 25 powder samples were extracted by Soxhlet Extraction and then separated into saturated hydrocarbons, aromatic hydrocarbons, asphaltic hydrocarbons, and non-hydrocarbons after using liquid column chromatography. GC analysis of the saturated hydrocarbons was conducted on an Agilent 7890A gas chromatograph instrument (Agilent Technologies Inc., Santa Clara, CA, USA) at China University of Geosciences (Wuhan, China). The oven temperature was set to an initial isothermal hold of 70 °C for 5 min, then ramped to 300 °C at 3 °C/min. GC-MS analysis was performed by an Agilent 7890 A-GC/5975C-MS instrument. Helium was a carrier gas at a 1.2 mL/min flow rate. The temperature program was from an initial isothermal hold of 60 °C for 5 min to 300 °C (hold 30 min) at a rate of 3 °C/min. Specific ions were monitored using specific ion monitoring functions and data acquisition systems. Then, a relative terpene and steroid abundance were obtained by measuring the corresponding peak areas, respectively.

## 4. Results

### 4.1. TOC and Rock-Eval Pyrolysis Data

The TOC and Rock-Eval pyrolysis data is useful to evaluate the quality of source rocks such as kerogen types, hydrocarbon generation potentials, and maturity [21,24]. The TOC, S<sub>1</sub> + S<sub>2</sub>, and HI values of the Yueguifeng Formation samples are in the range of 0.26–0.79 wt%, 0.27–4.29 mg HC/g rock, and 19–184.15 mg HC/g TOC (Table S1), respectively. Overall, the western region and the northeastern region have a lower average TOC content and a higher average HI value than other zones in Lishui Sag. The S<sub>1</sub> + S<sub>2</sub> values of source rocks in the western region are higher than those in the eastern region (Table S1; Figure 3).

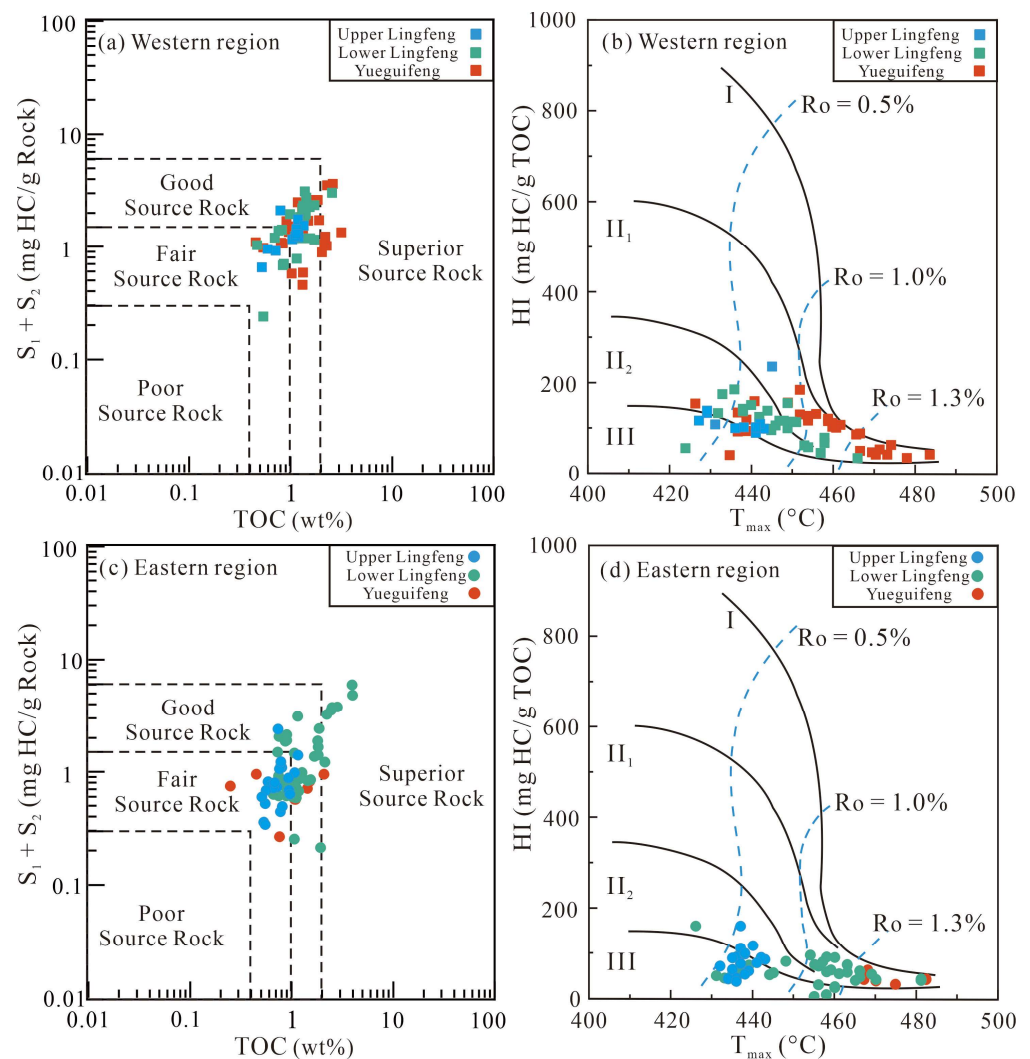


**Figure 3.** Variation of  $S_1 + S_2$  values vs. TOC values and hydrogen indexes vs.  $T_{max}$  values for source rock classifications of source rock quality and type, respectively. Upper Lingfeng = the upper member of Lingfeng Formation; lower Lingfeng = the lower member of Lingfeng Formation, Yueguifeng = Yuiguifeng Formation. (a,b) Organic matter abundance and kerogen types in the western region, respectively, (c,d) organic matter abundance and kerogen types in the western region, respectively.

The TOC,  $S_1 + S_2$ , and HI values of the lower member of Lingfeng Formation samples vary between 0.47 and 4.12 wt%, 0.54 and 3.02 mg HC/g rock, and 29 and 148.36 mg HC/g TOC (Table S1), respectively. On the whole, the TOC average content of the western region in Lishui is higher than that of the eastern region, and the  $S_1 + S_2$  and HI values in the south of the western region and the northeastern region are higher average than those of other zones (Table S1; Figure 3). The content of TOC in the upper member of Lingfeng Formation samples ranges from 0.52 to 5.70 wt%, with the  $S_1 + S_2$  values ranging from 0.52 to 0.81 mg HC/g rock. HI values vary between 47.98 and 240.28 mg HC/g TOC (Table S1; Figure 3).

$T_{max}$  is a key indicator for evaluating thermal maturity [51]. In general,  $T_{max}$  values are less than 435 °C, 435–470 °C, and higher than 470 °C for immature, mature, and overmature organic matter, respectively [44]. The samples of the Yueguifeng Formation have a wide  $T_{max}$  range of 434–481 °C, suggesting mature or overmature organic matter. The lower member of Lingfeng Formation samples also have a wide  $T_{max}$  range of 432–470 °C in the Lishui Sag, indicating that most samples are mature organic matter with a small number of immature samples. The upper member of Lingfeng Formation samples display a narrow

$T_{max}$  range of 434–445 °C in the northeastern region, indicating mature organic matter. In general, the maturity of source rocks in the Yueguifeng Formation is higher than those in the Lingfeng Formation (Table S1; Figure 3).

4.2. Major and Trace Elements Data

Major and trace elements are vital indicators for sedimentary environment reconstruction [21–23,52]. The element ratios of Sr/Ba, B/Ga, V/(V + Ni), Cl, Sr/Cu, Fe/Mn, and  $Mo_{EF}/U_{EF}$  have ranges of 0.03 to 2.23, 1.17 to 4.92, 0.62 to 0.96, 0.19 to 0.89, 3.90 to 37.52, 25.19 to 247.17, 1.01 to 4.85, with their averages of 0.53, 3.43, 0.78, 0.41, 14.53, 109.01, 2.14, respectively (Table S2). Compared with the lower Yueguifeng Formation, the samples in the upper member of Lingfeng Formation have higher Sr/Ba, B/Ga, and Sr/Cu ratios but lower V/(V + Ni), Cl, and Fe/Mn values (Table S2; Figure 4a–f).

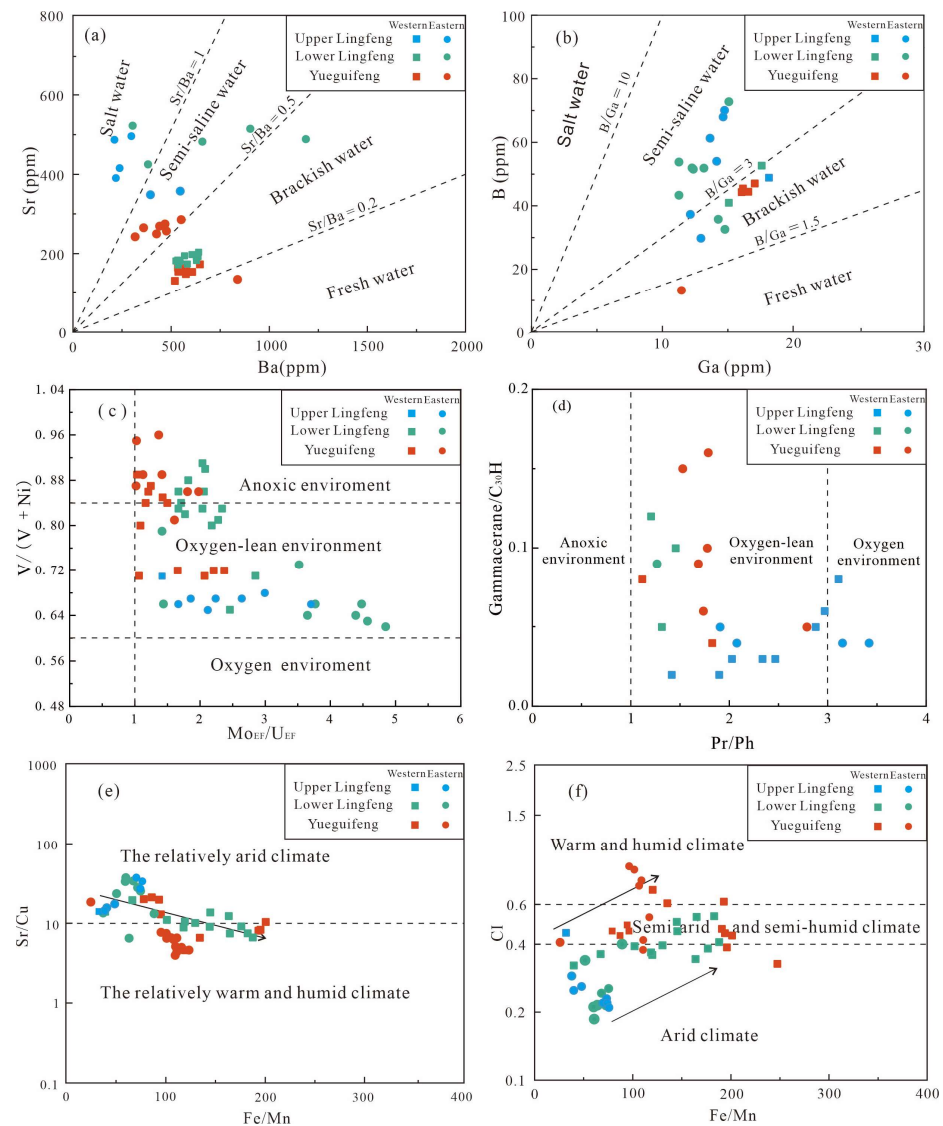


**Figure 4.** Diagrams of geochemical indicators in the Lishui Sag, showing the depositional environments. Note: CI (Climate Index) =  $(Fe + Mn + Cr + V + Co + Ni) / (Ca + Mg + Sr + Ba + K + Na)$ ; Enrichment factors (EF) were calculated using the formula  $X_{EF} = [(X/Al)_{sample} / (X/Al)_{PAAS}]$ , where X represents the specific trace element (e.g., Mo) and PAAS stands for Post-Archean average Australian shales [53]. Upper Lingfeng = the upper member of Lingfeng Formation; lower Lingfeng = the lower member of Lingfeng Formation, Yueguifeng = Yuiguifeng Formation. (a,b) Display of the paleosalinity; (c,d) exhibition of the paleoredox conditions; (e,f) presentation of the paleoclimate.

### 4.3. GC and GC-MS Analysis Results

The GC analysis results show that the samples in the Yueguifeng Formation have Pr/Ph ratios ranging from 1.01 to 2.21, Pr/n-C<sub>17</sub> ratios ranging from 0.74 to 2.36, and Ph/n-C<sub>18</sub> ratios ranging from 0.17 to 1.14 (Table S3; Figures 4d, 5e–h and 6a). Overall, the samples in the lower member of Lingfeng Formation show lower Pr/Ph ratios (0.14–1.57) and Pr/n-C<sub>17</sub> ratios (0.79–1.83) but higher Ph/n-C<sub>18</sub> ratios (0.19–6.92) (Table S3; Figures 4d, 5a–d and 6a). The samples in the upper member of Lingfeng Formation display great differences in GC data from the lower member with their Pr/Ph, Pr/n-C<sub>17</sub>, and Ph/n-C<sub>18</sub> ratios at 1.12 to 2.79, 0.17 to 3.16, and 0.08 to 5.57, respectively (Table S3; Figures 4d and 5). Additionally, the samples from the southern region of the eastern region exhibit a higher abundance of short-chain *n*-alkanes (Figure 5d,h). In contrast, the samples from the northeastern region predominantly contain short- to middle-chain *n*-alkanes, while the samples from the western region show a predominance of middle- to long-chain *n*-alkanes (Figure 5).

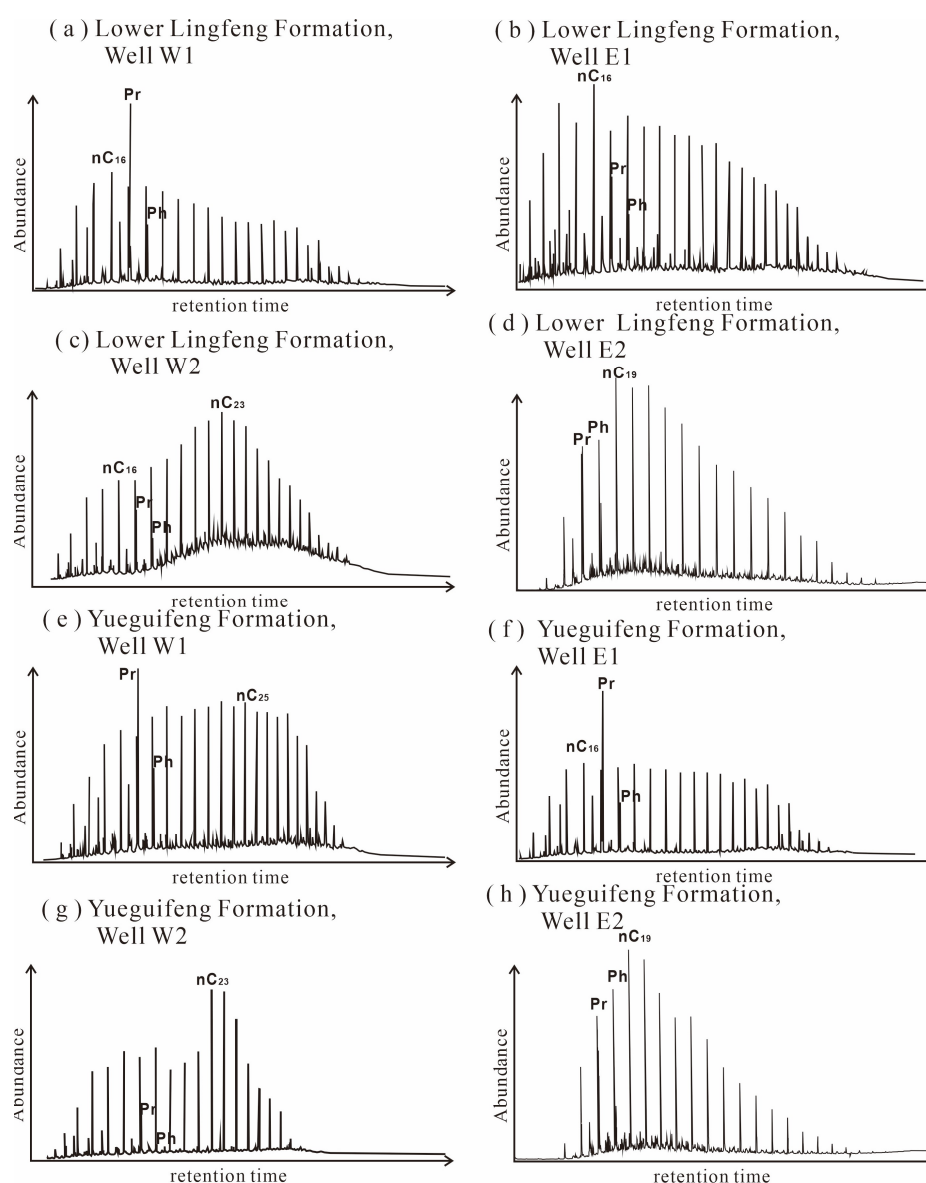


**Figure 5.** Gas chromatograms of saturated hydrocarbon fractions for source rocks in the Lishui Sag. Upper Lingfeng Formation = the upper member of Lingfeng Formation; lower Lingfeng Formation = the lower member of Lingfeng Formation.

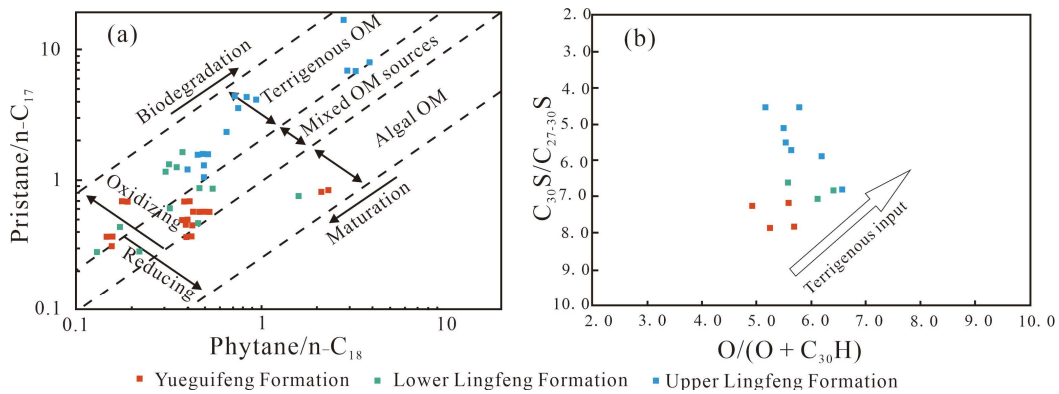


**Figure 6.** Biomarkers of the source rocks in the Lishui Sag, showing the origin of organic matter and the depositional environments. Note: (a) is derived from our measured data; (b) data is from Li et al., 2019 [45]; OM represents organic matter. Upper Lingfeng Formation = the upper member of Lingfeng Formation; lower Lingfeng Formation = the lower member of Lingfeng Formation.

The GC-MS results display wide variations in the abundances of gammacerane, C<sub>27</sub>R, C<sub>28</sub>R, and C<sub>29</sub>R, and narrow variations in the abundances of 17α(H)-norhopane/17α(H)-hopane (C<sub>29</sub>H/C<sub>30</sub>H) (Table S3; Figures 4d and 7). The average of C<sub>27</sub>R sterane contents shows an increasing tendency from the Yueguifeng Formation (27%) to the Lingfeng Formation (30%) (Figure 7). On the contrary, from the Yueguifeng Formation to the Lingfeng Formation, the average values of C<sub>29</sub>R sterane decreased from 51% to 47% (Figure 7). In addition, comparing the data of the eastern region, the samples of the western region in the Yueguifeng and lower member of Lingfeng Formations have higher average C<sub>29</sub>R sterane contents than C<sub>28</sub>R sterane contents (Figure 7).

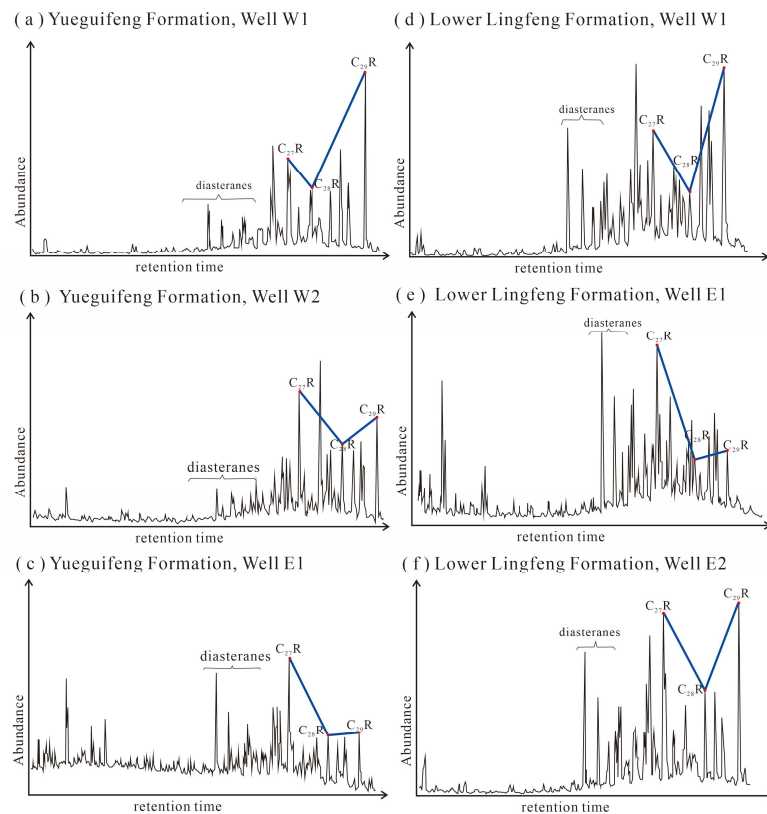


**Figure 7.** Saturated hydrocarbon sterane *m/z* 217 mass chromatogram of hydrocarbon source rocks in the Lishui Sag. Upper Lingfeng Formation = the upper member of Lingfeng Formation; lower Lingfeng Formation = the lower member of Lingfeng Formation.

### 5. Discussion

#### 5.1. Paleoenvironmental Evolution in the Paleocene (66~59.2 Ma)

In the early Paleocene, the Lishui Sag had multiple isolated depocenters divided by regional uplifts (e.g., Minzhe, Lingfeng, and Yandang Uplifts), providing conditions for the development of lacustrine source rocks. By contrast, in the middle Paleocene (62~61 Ma), transgression from the southeast transformed the restricted lacustrine environment into an open shallow marine environment. Widespread marine source rocks were deposited in this paleoenvironmental background (Figure 8b,c) [37,46]. Therefore, this study suggests that the Lishui Sag transitioned from a closed lake to an open-marine environment in the Paleocene (Figure 8a–c), which is consistent with the conclusion in the previous studies that there was an increase in global sea level accompanied by a gradual warming trend in the Earth’s climate in the Paleocene [39,46,50,54].

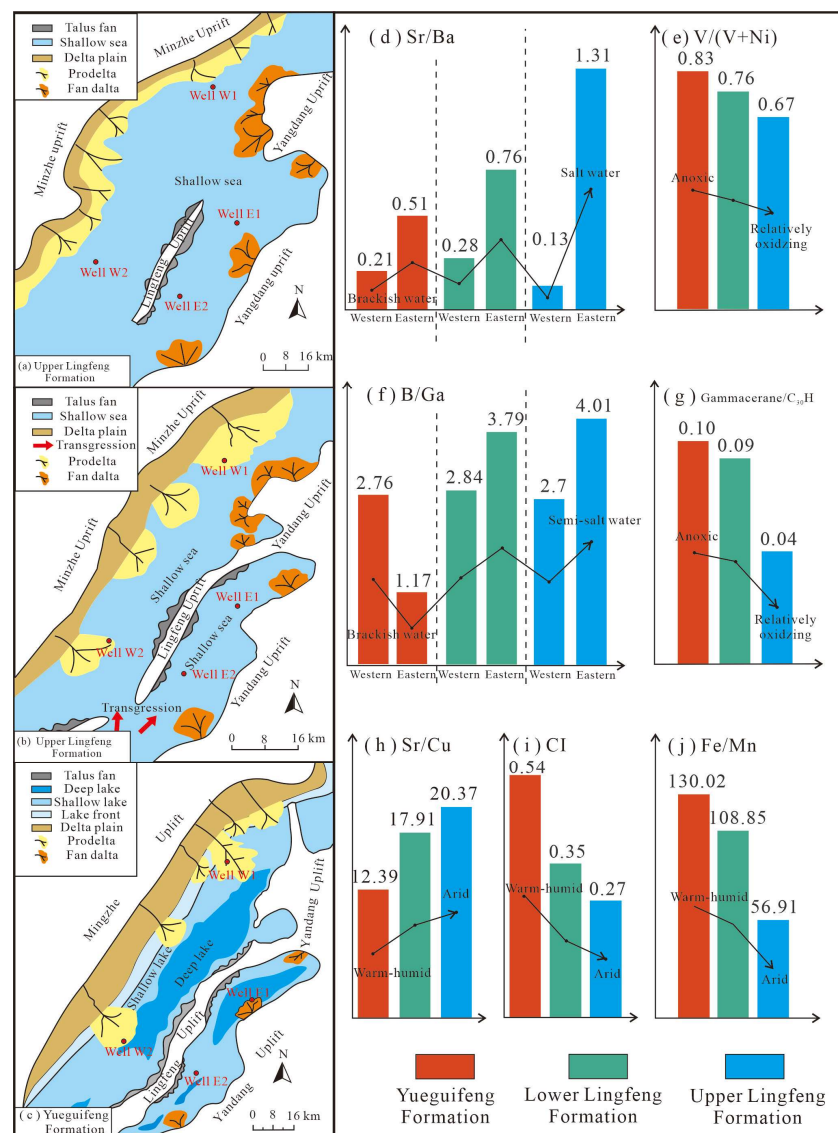


**Figure 8.** Sedimentary facies chart in the Lishui Sag with average values of each paleoenvironmental indicator. The sedimentary facies chart was modified after Zhang et al., 2023; Sun et al., 2020, and Zhang et al., 2015 [33,37,55]. Upper Lingfeng Formation = the upper member of Lingfeng Formation; lower Lingfeng Formation = the lower member of Lingfeng. (a–c) The transition from a closed lake to an open shallow sea in the sedimentary environment; (d,e) the variations in paleosalinity and differences between the eastern and western region; (f,g) the alterations in paleoredox conditions; (h–j) the changes in paleoclimate.

The paleosalinity data further confirms the transition from a closed lake to an open marine environment [42,56]. The Sr/Ba and B/Ga ratios can be used to indicate the paleosalinity, with higher specific values suggesting higher salinity [57,58]. The ratios of Sr/Ba and B/Ga show gradually increasing trends from the Yueguifeng Formation to the upper member of Lingfeng Formation, reflecting a transition of paleosalinity from freshwater-brackish water to semi-saline or even saline conditions in the paleoenvironmental evolution processes (Figures 4a,b and 8d,f). This is consistent with the conclusions in the previous studies [59]. It is worth noting that the average Sr/Ba and B/Ga ratios in the eastern region are higher than those of the western region, indicating that the water in the eastern region is saltier than that in the western region, which may be related to more influences of seawater in the eastern region (Figure 8d,f).

The redox condition plays an important role in the development of source rocks. Higher values of  $V/(V + Ni)$  and lower Pr/Ph ratios indicate a relatively reducing environment in the water [51,60,61]. The  $V/(V + Ni)$  ratios in the samples of Yueguifeng, lower member of Lingfeng, and upper member of Lingfeng formations are in ranges of 0.71–0.96 (averaging 0.83), 0.62–0.90 (averaging 0.76), and 0.65–0.71 (averaging 0.67), respectively. Moreover, the average ratios of Pr/Ph show gradually increasing trends from 1.78 in the lower Yueguifeng Formation to 2.56 in the upper member of Lingfeng Formation. These ratios suggest that Lishui Sag experienced a transition from an anoxic into a relatively oxidizing environment (Figures 4c,d and 8e). In addition, high gammacerane levels are a significant biomarker produced in a reducing environment [55,62]. The observed declines in gammacerane index (gammacerane/ $C_{30}$  hopane), with the regular stair-step progression of  $C_{31}$ – $C_{35}$  homohopanes,  $C_{29}H/C_{30}H < 1$  and  $Mo_{EF}/U_{EF} > 1$  further support the above conclusion (Table S3; Figures 4c, 7a, 8g and 9a–c) [38]. This transition in the Lishui Sag is associated with climate and depositional system changes, resulting in fluctuating water inflow that transported more dissolved oxygen to the coastal zones and created a more oxidizing environment [41].

Paleoclimate is a crucial determinant in paleoenvironmental evolution, and certain indicators can provide valuable insights [44,63]. For instance, a lower Sr/Cu ratio or higher Fe/Mn and CI values can suggest a shift towards a warmer and more humid climate [64–67]. Compared with the Lingfeng Formation, the samples in the Yueguifeng Formation are marked by higher values of Fe/Mn and CI, but lower values of Sr/Cu ratios, suggesting a transition from a warm-humid to a relatively arid climate in the Paleocene (66–59.2 Ma, Figures 4e,f and 8h–j). Previous studies suggest that, in the Yueguifeng Formation depositional period, a warm climate (27–30 °C) with limited evaporation created favorable conditions for the proliferation of plants and microfauna in the enclosed lacustrine environment evidenced by paleontological data (e.g., Pollen, Algae, and Ostracoda) [39]. In contrast, during the Lingfeng Formation depositional period, a warmer climate (30 °C) accompanied by relatively sufficient rainfall promoted the thriving of gymnosperms and angiosperms in the relatively open bay setting [39]. Liu et al. (2005) [68] also point out that the Lingfeng Formation was deposited in a relatively arid-hot climate. Overall, the climate in Lishui Sag progressively shifted towards warmer-drier conditions, which is consistent with the context of global climate change in the Paleocene [54], which had a further effect on the transformation of the ecosystem.

The paleoenvironment evolution plays an effect on the chemical component and terrigenous input, which can be recorded by the deposition of mudstones in a basin [67,69–72]. Some pyrites and rare bioturbations are observed in the core samples of the Yueguifeng Formation, indicating a strong-reducing environment (Figure 10b,c). By contrast, the mudstones in the upper member of Lingfeng Formation are marked by increased bioturbation, lighter color, and altered structure, indicating significant alterations in the paleoenvironment during its depositional period (Figure 10a). The rapid paleoenvironment (especially paleoclimatic changes) changes resulted in a greater input of terrigenous organic matter and the intensity of ocean currents, which further led to an increase the nutrition regionally [73–75]. The organic matter sources in the Lishui Sag exhibit a gradual increase in

terrigenous sources, which is further evidenced by the biomarker parameters of the Pr/n-C<sub>17</sub>, Ph/n-C<sub>18</sub>, and the decreasing  $\sum C_{21-} / \sum C_{21+}$  ratios, as well as Carbon Preference Index (CPI) values (Figure 6 and Table S3). In addition, it is worth noting that the western region has higher terrigenous organic matter input than those in the eastern region (Figures 5 and 6) [29]. For instance, the *n*-alkanes of samples in the western region appear in a predominance of middle- to long-chain *n*-alkanes with a higher proportion of homologs (C<sub>29</sub>R) than steranes (C<sub>27</sub>R) (Figures 5 and 6). By contrast, the samples of the eastern region show a higher abundance of short- to middle-chain *n*-alkanes and a lower proportion of homologs (C<sub>29</sub>R) than steranes (C<sub>27</sub>R).

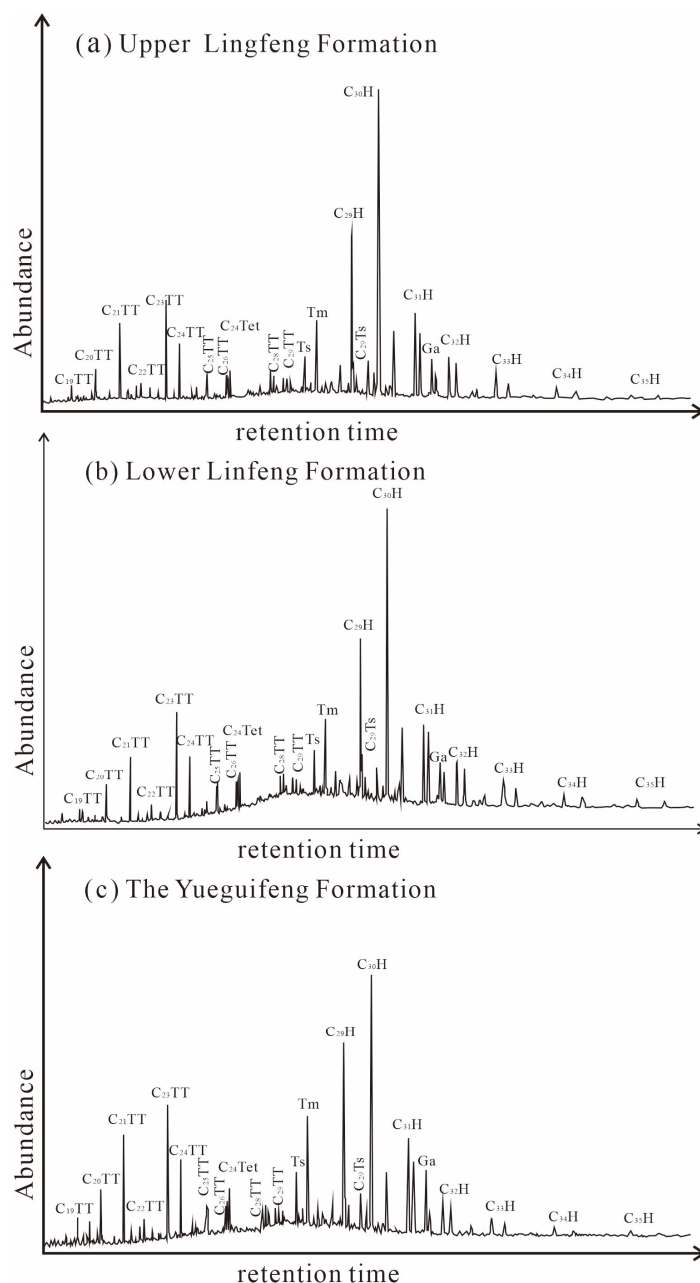


**Figure 9.** Representative saturated fraction mass chromatograms ( $m/z$  191) of source rocks in the Lishui Sag, showing the distributions of terpenes. C<sub>20</sub>TT–C<sub>29</sub>TT: tricyclic terpenes with different carbon numbers; C<sub>29</sub>H: C<sub>29</sub> hopane; C<sub>30</sub>H: C<sub>30</sub> hopane; Ts: C<sub>27</sub>18 $\alpha$ (H)-22, 29, 30-trinorhopane; Tm: C<sub>27</sub>17 $\alpha$ (H)-22, 29, 30-trinorhopane. Note: data is from Li et al., 2019 [45]. Upper Lingfeng Formation = the upper member of Lingfeng Formation; lower Lingfeng Formation = the lower member of Lingfeng Formation.

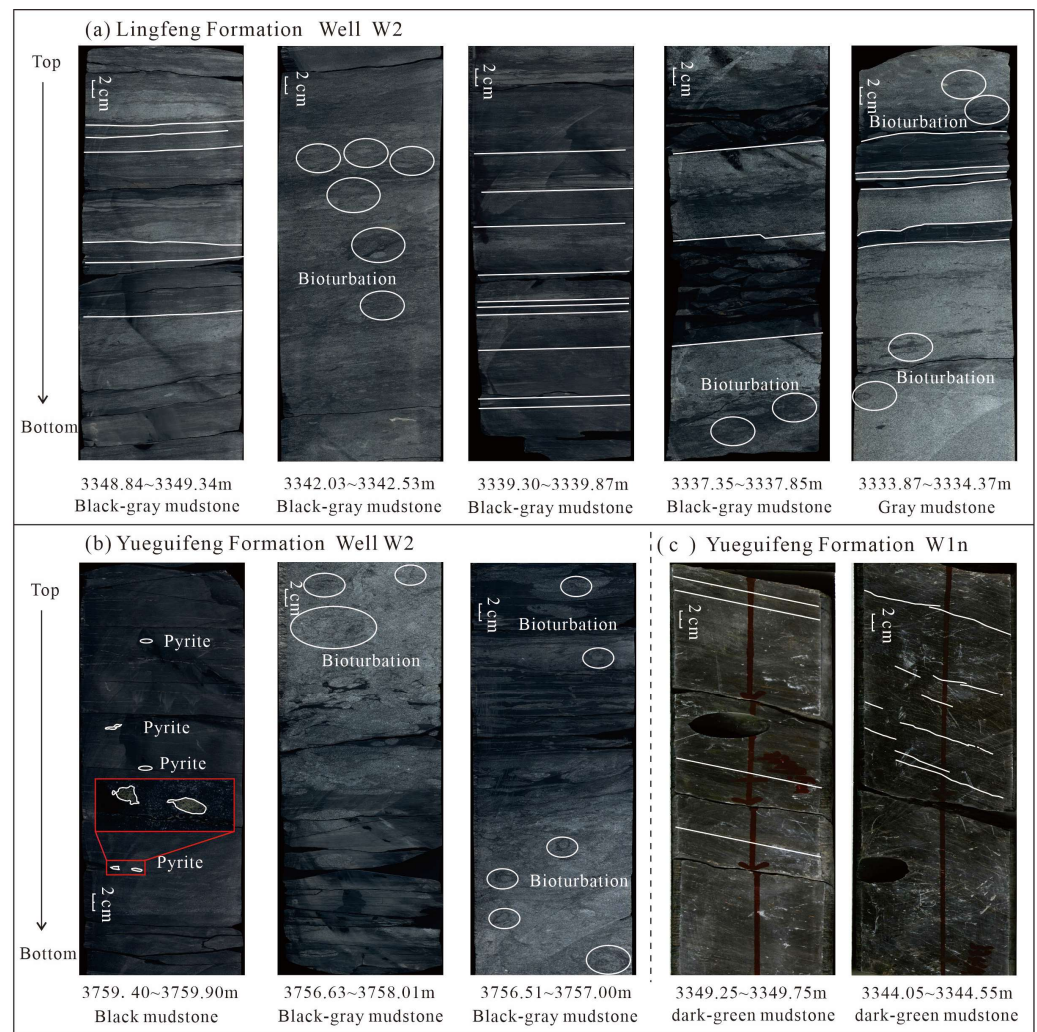


**Figure 10.** Mudstone core samples from Well W2 and W1n in the Yueguifeng Formation and Lingfeng Formation. (a) 3348.84~3349.34 m, 3342.03~3342.53 m, 3339.30~3339.87 m, 3337.35~3337.85 m, 3333.87~3334.37 m (from left to right) in Well L1, massive grey silty and white mudstones with bioturbation and parallel bedding structures; (b) 3759.40~3759.90 m, 3756.63~3758.01 m, 3756.51~3757.00 m (from left to right) in Well L1, massive black mudstones with small amount of pyrite and obvious bioturbation. (c) 3349.25~3349.75 m, 3344.05~3344.55 m in Well 1<sub>n</sub>, with massive dark green mudstones. Fine horizontal lamination structures are also visible. Please note that Well 1<sub>n</sub> is inclined, which affects its bedding structures' orientation. Pyrite is a mineral that forms under strongly reduced conditions [67].

The variation in the source of organic matter is strongly influenced by changes in relative sea level and paleobathymetry, which are critical in determining the composition and characteristics of plant communities [76]. During the middle Paleocene (61.6~59.2 Ma), the paleobathymetry gradually rose in the eastern region while it decreased in the western region [39]. This led to the formation of extensive shallow swampy zones in the western region, facilitated by the combination of decreasing water depth and the presence of a trench-like landform (Figure 1d). The shallow waters in these zones received an influx of river water, maintaining a suitable salinity for plant growth and leading to an increase in terrestrial organic matter input. On the other hand, the eastern region, being located in a more distal position (Figure 9a–c), experienced a slower increase in terrestrial organic matter in the progressively opening water environment. These factors contribute to the observed trend of increasing terrestrial organic matter and the disparity between the eastern and western regions.

In summary, the Lishui Sag transitioned from an enclosed freshwater lake to an open shallow marine system in the Paleocene, with a shift from a warm-humid to an arid climate. During this process, the aquatic environment in the basin was gradually becoming oxidized, with a gradual increase in salinity and terrigenous organic matter content. Compared to the eastern region, the western region had higher terrigenous organic matter input but lower salinity. Changes in the water sedimentary system and paleoenvironment or different geographical locations have a significant impact on the variations in organic matter types. It is noteworthy that the climate and sea level fluctuations (Figure 2) observed in the study area align with the broad global trends during this period [50,54].

### 5.2. Accumulation Factors of Organic Matter in a Saline Condition Rift Basin

The supply and preservation of organic material are the two key factors in the accumulation of organic matter [6,8]. The supply of organic matter is controlled by several factors such as climate, salinity, water depth, and stability, as well as the input of terrestrial and aquatic materials. Preservation of organic matter is influenced by factors including water stability, deposition rate, and redox conditions [64,77,78]. Previous studies suggested that a warm and humid climate with low salinity contributes to biogenic richness, which provides organisms with sufficient nutrients from terrigenous influx [79]. The correlation between TOC, major, and trace elements in the Lishui Sag provide further confirmation. Specifically, a negative correlation between TOC and Sr/Cu (Figure 11e), as well as a positive correlation between TOC and CI values are observed (Figure 11f), suggesting that a warm-humid climate promoted organic matter enrichment. Moreover, the ratios of Sr/Ba and B/Ga show positive correlations with TOC contents (Figure 11a,b), indicating that a specific salinity level also contributed to the enrichment of organic matter. This is consistent with the phenomenon in the Dongpu Depression, Bohai Bay Basin that brackish water is beneficial to TOC enrichment [64,77]. In addition to a sufficient supply of organic matter, depositional factors, such as the degradation and dilution of organic matter, can also affect its preservation [80]. TOC is positively correlated with the V/(V + Ni) ratio (Figure 11c) but negatively correlated with the Pr/Ph ratios (Figure 11d), indicating that the reducing environment was critical for the preservation of organic matter.

The previous studies documented that the Lishui Sag experienced a great decrease in tectonic subsidence in the Paleocene [33,80], which influenced terrigenous organic matter input and depositional evolution (Figures 6, 7 and 9). In the early period (66–61.6 Ma), the Lishui Sag was marked by an underfilled lake with a low material supply rate but a high subsidence rate, resulting in the occurrence of multiple isolated subsidence centers [41,48]. Some studies suggest that extensive magmatic activity occurred in the East China Sea from the Mesozoic to Early Cenozoic, contributing to the primary source of neutral or acidic magmatic rocks nearby for the Paleocene provenance of the Lishui Sag [37,46,81]. Volcanic activity increased salinity and enriched nutrient elements like Ca, Si, and Mg in the Lishui Sag [82,83]. Therefore, during the depositional period of the Yueguifeng Formation, the warm and humid climate enhanced weathering strength and resulted in a large input of terrigenous and algal organic matter.

The presence of favorable preservation conditions and abundant supply of organic matter led to the formation of high-quality lacustrine source rocks in the Yueguifeng Formation (Figure 12c). In the case of closed and underfilled lakes, combined with high water influxes during wet climates, the low area/depth ratio and deepening of the water column promoted the inhibition of efficient water mixing and the establishment of stable anoxic water column stratification [41,84–86]. The anoxic environment is further confirmed by high V/(V + Ni), low Pr/Ph, and high gammacerane/C<sub>30</sub> hopane values. Additionally, the occurrence of abundant pyrites in the core samples also indicates the presence of an anoxic environment. Consequently, high-quality lacustrine source rocks are mainly found in the deep lakes of the western and northeastern regions of the Lishui Sag (Figure 12c).

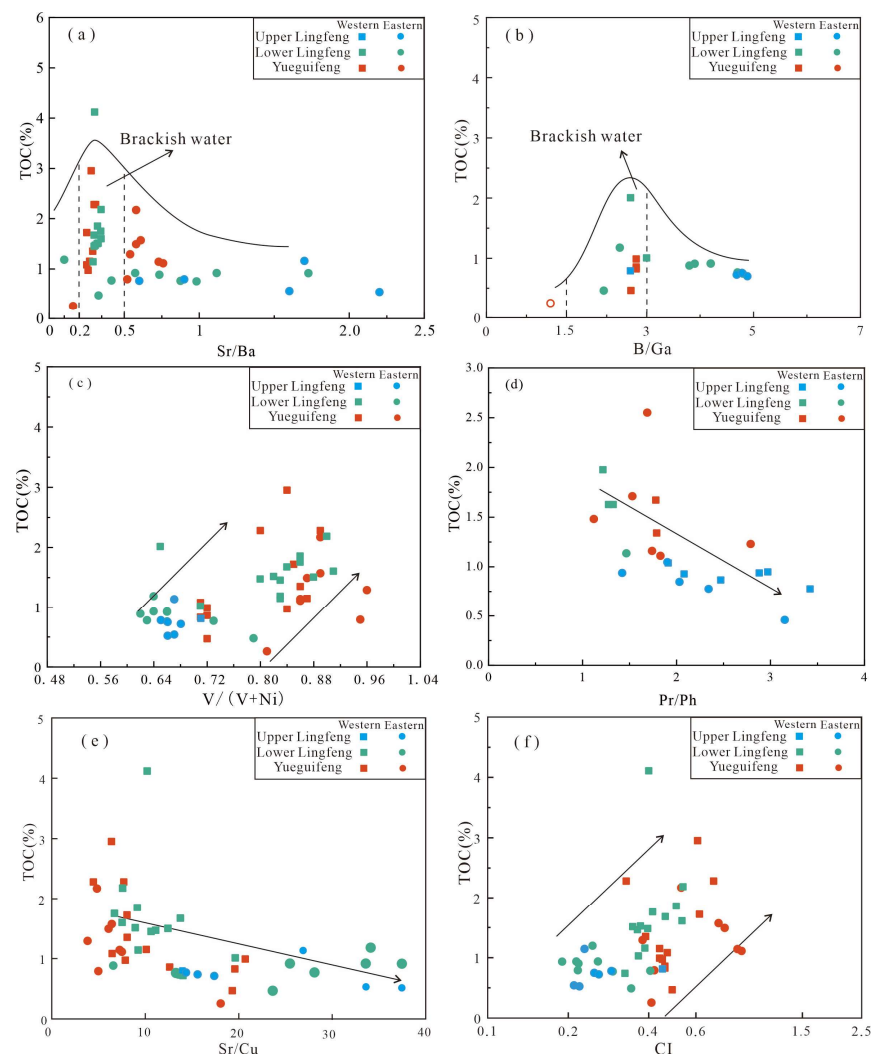


**Figure 11.** Correlation plot between paleoenvironmental indicators and TOC in Lishui Sag, (a,b) The correlation plot between paleosalinity and TOC; (c,d) the correlation plot between paleo-redox condition and TOC; (e,f) the correlation plot between paleoclimate and TOC. Upper Lingfeng = the upper member of Lingfeng Formation; lower Lingfeng = the lower member of Lingfeng Formation, Yueguifeng = Yuiguifeng Formation.

In the late period (61.6~59.2 Ma), the subsidence rate was significantly lower than the sediment supply rate (namely a filled or overfilled basin) [38,41,46]. Zhang et al. (2023) suggested simultaneous occurrences of foraminifera and dinoflagellates around 61 Ma, indicating the transition from lacustrine to marine facies in the lower member of Lingfeng Formation [37]. Despite the gradual warming and aridification of the climate during the lower member of Lingfeng Formation’s depositional period, the continuous increase in terrestrial organic matter has led to a sustained, relatively high input of material supply (this aspect was discussed in Section 5.1). However, relatively oxidizing preservation conditions result in a decline in organic matter abundance and a restricted distribution of source rocks (Figure 3a,c). In addition, extensive shallow swampy zones emerged in the delta of the western region, characterized by low salinity water conditions. These zones provided favorable conditions for the accumulation of both terrestrial and algal organic matter (Figure 13b). As a result, marine source rocks are primarily concentrated in the western region of the lower member of Lingfeng Formation.

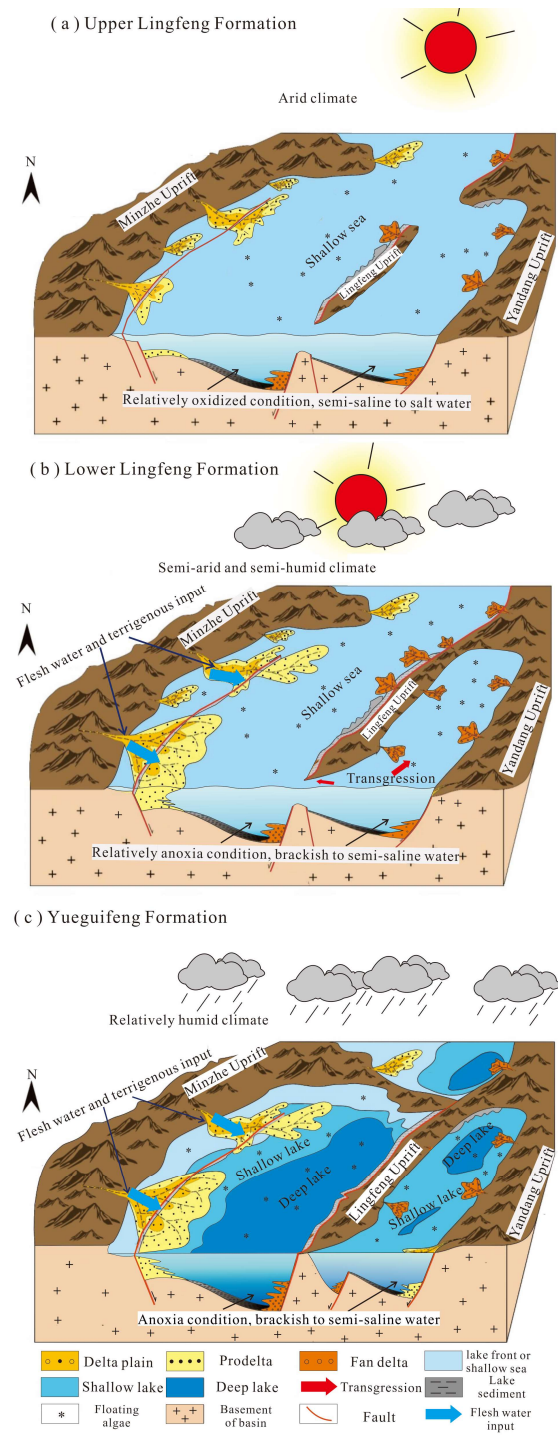


**Figure 12.** Two source rock deposition models are established based on tectonic setting and climate change in the Lishui Sag. Upper Lingfeng Formation = the upper member of Lingfeng Formation; lower Lingfeng Formation = the lower member of Lingfeng Formation.

During the depositional period of the upper member of Lingfeng Formation, the Lishui Sag is marked by an open ocean, characterized by a relatively hot and dry climate with relatively high salinity water. The fluctuating water inflow, along with an increase in dissolved oxygen, transported oxygenated water to the shallow coastal marine or paralic zones, resulting in a relatively oxidized environment [41]. This is further supported by high ratios of biomarkers such as  $C_{19} T/C_{23} T$ ,  $C_{20} T/C_{23} T$ , and  $C_{24} Tet/C_{26} T$  in this study. Compared to the Yueguifeng Formation, the Lingfeng Formation has

unfavorable conditions for the growth of plants, algae, and the preservation of organic matter. As a result, only low-quality source rocks were deposited in the upper member of Lingfeng Formation.

### 5.3. Implications for Hydrocarbon Exploration in the Lishui Depression

To evaluate the quality of hydrocarbon generation potential, many parameters should be considered such as organic abundance, kerogen type, and thermal maturity of source rocks [87,88]. This research evaluated the hydrocarbon generation potential of source rocks using TOC and the Rock-Eval pyrolysis data.

The majority of mudstone samples in this study are categorized as fair to good source rocks, with a small proportion as superior source rocks (Figure 3a,c). The organic abundance in the upper member of Lingfeng Formation is lower than that in the Yueguifeng and lower member of Lingfeng formations (Figures 3a,c and 13). Most samples in the Yueguifeng and lower member of Lingfeng formations fall into the type II<sub>1</sub>–II<sub>2</sub> kerogen zone, with relatively high hydrocarbon generation potential (average HI values of 91.52 and 87.73 mg HC/g TOC, respectively) (Figure 3b,d). By contrast, the samples from the upper member of Lingfeng Formation are predominantly composed of type III kerogen, characterized by a higher hydrocarbon generation potential as indicated by an average HI value of 100.94 mg HC/g TOC (Figure 3b,d). Moreover, most samples in the Yueguifeng and lower member of Lingfeng formations are positioned within the mature to overmature zones. In contrast, the samples from the upper member of Lingfeng Formation have reached a state of maturity (Figure 3b,d). On the whole, the thermal maturity of samples from the Yueguifeng and lower member of Lingfeng formations is higher than those in the upper member of Lingfeng Formation. In addition, compared with the overlying strata, the samples of the Yueguifeng Formation show the highest hydrocarbon generation potential and maturity interpreted by TOC and the Rock-Eval data (Figures 3b and 13), which provides basic conditions for the LS36-A gas field [41,89].

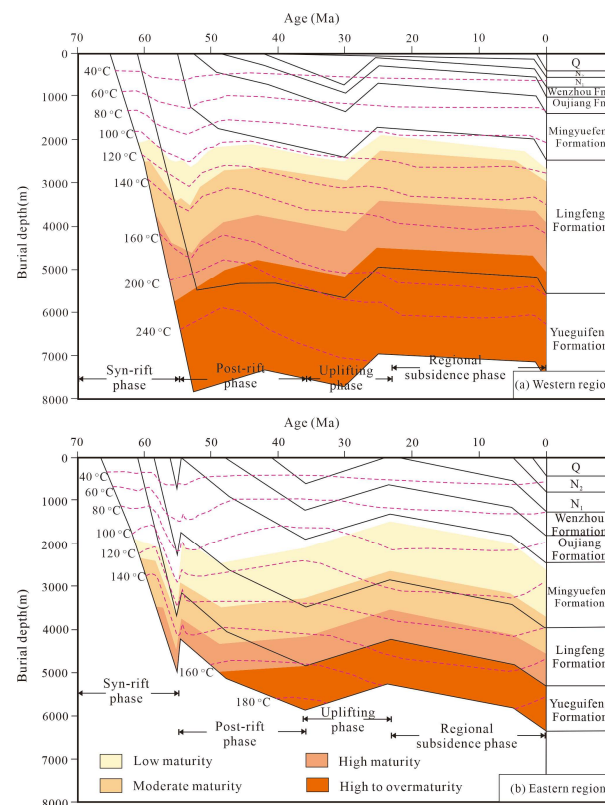


**Figure 13.** Burial-thermal histories in the Lishui Sag (Modified after Li et al., 2019; Lei et al., 2021 [45,90]). Note: Fm. = Formation.

The high-quality source rocks in the Yueguifeng Formation are mainly distributed in the western and northeastern regions of the Lishui Sag due to their location in semi-deep or deep lakes, offering ample reducing storage space for preserving mixed sources of organic matter. As a result, compared to other areas, source rocks in these areas exhibit greater thickness and higher organic abundance (Figure 3). Li et al. (2019) suggested that the relatively high-quality source rocks in the Lingfeng Formation were mainly concentrated in the western region [45]. Currently, a significant gas field (namely LS36-A gas field) and several oil- and gas-bearing structures have been discovered in the western region [34,35]. Meanwhile, the source rocks in the northeastern region of the Lishui Sag show high organic abundance and hydrocarbon potential. For instance, the average TOC contents is 1.39, even higher than that of the western region (average: 1.18). In addition, most samples have reached gas potential due to their relatively deep burial (Figure 3) [45]. Therefore, the source rocks in the northeastern part of Lishui Sag exhibit large thickness, high quality, and high maturity [45]. Considering that the exploration and development in this area remain limited (Figure 3), we suggest that the northeast region area should be considered as the next target for exploration and development.

## 6. Conclusions

Based on our bulk geochemical data (e.g., TOC, major and trace elements, and biomarker data), the following conclusions can be drawn from our reconstruction of the paleoenvironment in the Paleocene (66~59.2 Ma) and clarification of the mechanism of organic matter enrichment in the Lishui Sag, East China Sea.

- (1) During the Paleocene, the Lishui Sag transformed from a closed lake to an open-marine environment, accompanied by a shift from warm-humid to arid climate conditions. Trace elements and biomarkers further support this transition, indicating a gradual oxidation process and an increase in salinity levels.
- (2) In the early Paleocene, lacustrine hydrocarbon source rocks in the Yueguifeng Formation formed in a warm-humid climate and brackish water environment, preserving a significant amount of mixed organic matter under anoxic conditions. In the late stage, marine hydrocarbon source rocks in the Lingfeng Formation developed under relatively arid and oxidizing conditions, with increased input of terrestrial organic matter and water salinity.
- (3) The source rocks in the Yueguifeng and lower member of Lingfeng formations are dominated by Type II kerogen, while Type III kerogen is predominant in the upper member of Lingfeng Formation. The majority of source rocks have reached maturity and the threshold for hydrocarbon generation. Additionally, the thermal maturity of samples from the Yueguifeng Formation is higher compared to the samples from the Lingfeng Formation. Biomarker results reveal a transition from a blend of aquatic and terrestrial organic matter sources to a greater inflow of terrestrial organic matter in the source rocks.
- (4) The northeastern part of Lishui Sag is recommended as a significant target zone for future exploration. The source rocks in this region have reached the gas-generating threshold and further exploration should be advised to intensify efforts to search gas fields.

**Supplementary Materials:** The following supporting information can be downloaded at: <https://www.mdpi.com/article/10.3390/jmse11122341/s1>, Table S1: Rock-Eval pyrolysis, TOC data, and derived parameters for the source rocks in the Lishui Sag,  $HI = S_2 \times 100/TOC$ ; Table S2: The paleoenvironmental element indexes of the Lishui Sag; Table S3: Biomarker Parameters of source rocks in the Lishui Sag.

**Author Contributions:** Conceptualization, E.L. and J.Z. (Junming Zhan); methodology, E.L., J.Z. (Junming Zhan) and Q.Z.; software, Y.C., Y.Z. and Y.J.; validation, E.L., J.Z. (Junming Zhan) and Q.Z.; formal analysis, E.L.; investigation, J.Z. (Junming Zhan) and Q.Z.; resources, E.L.; data curation, E.L. and S.C.; writing—original draft preparation, J.Z. (Junming Zhan); writing—review and

editing, E.L.; visualization, J.Z. (Jialin Zhong) and P.Y.; supervision, E.L. and Q.Z.; project administration, E.L.; funding acquisition, E.L. All authors have read and agreed to the published version of the manuscript.

**Funding:** This research was funded by the National Natural Science Foundation of China (Nos. 42072142, 41702121). We thank the reviewers for reviewing this manuscript and the editor for editorial handling.

**Institutional Review Board Statement:** Not applicable.

**Informed Consent Statement:** Not applicable.

**Data Availability Statement:** The data presented in this study are available on request from the corresponding author.

**Acknowledgments:** We appreciate the Shanghai Branch of CNOOC (China) Co., Ltd. for providing the data and permission to publish this paper. We are also very grateful to the reviewers and editors for their contributions to improving this paper.

**Conflicts of Interest:** The authors declare no conflict of interest.

## References

- Cheng, D.W.; Zhou, C.M.; Zhang, Z.J.; Yuan, X.J.; Liu, Y.H.; Chen, X.Y. Paleo-environment reconstruction of the middle Permian Lucaogou Formation, southeastern Junggar Basin, NW China: Implications for the mechanism of organic matter enrichment in an ancient lake. *J. Earth Sci.* **2022**, *33*, 963–976. [[CrossRef](#)]
- Tyson, R.V. *Sedimentary Organic Matter: Organic Facies and Palynofacies*; Springer Science & Business Media: Berlin, Germany, 2012.
- Cirilli, S.; Simonetta, N.; Gugliotti, L.; Frixia, A. Palynostratigraphy and palynofacies of the Upper Triassic Streppenosa Formation (SE Sicily, Italy) and inference on the main controlling factors in the organic rich shale deposition. *Rev. Palaeobot.* **2015**, *218*, 67–79. [[CrossRef](#)]
- Playford, G.; Hashemi, H.; Wicander, R. The palynostratigraphy of the Lower Carboniferous (middle Tournaisian–upper Viséan) Shishtu Formation from the Howz-e-Dorah section, southeast Tabas, central Iranian Basin. *Palynology* **2017**, *40*, 247–263. [[CrossRef](#)]
- Zhu, G.Y.; Jin, Q.; Zhang, S.C.; Dai, J.X.; Wang, G.M.; Zhang, L.H.; Li, J. Characteristics and origin of deep lake oil shale of the Shahejie Formation of Paleogene in Dongying Sag, Jiyang Depression. *Palaeogeography* **2005**, *7*, 59–69.
- Gallego-Torres, D.; Martínez-Ruiz, F.; Paytan, A.; Jiménez-Espejo, F.J.; Ortega-Huertas, M. Pliocene-Holocene evolution of depositional conditions in the eastern Mediterranean: Role of anoxia vs. productivity at time of sapropel deposition. *Palaeogeography Palaeoclimatol. Palaeoecol.* **2007**, *246*, 424–439. [[CrossRef](#)]
- Xu, J.J.; Liu, Z.J.; Bechtel, A.; Meng, Q.T.; Sun, P.C.; Jia, J.L.; Cheng, L.J.; Song, Y. Basin evolution and oil shale deposition during Upper Cretaceous in the Songliao Basin (NE China): Implications from sequence stratigraphy and geochemistry. *Int. J. Coal Geol.* **2015**, *149*, 9–23. [[CrossRef](#)]
- Pedersen, T.F.; Calvert, S.E. Anoxia vs. productivity: What controls the formation of organic-carbon-rich sediments and sedimentary rocks?: Reply (1). *AAPG Bull.* **1991**, *75*, 500–501. [[CrossRef](#)]
- Zhang, S.C.; Zhang, B.M.; Bian, L.Z.; Jin, Z.J.; Wang, D.R.; Zhang, X.Y.; Gao, Z.Y.; Chen, J.F. Development constraints of marine source rocks in China. *Earth Sci. Front.* **2005**, *12*, 39–48.
- Demaison, G.J.; Moore, G.T. Anoxic environments and oil source bed genesis. *Org. Geochem.* **1980**, *2*, 9–31. [[CrossRef](#)]
- Arthur, M.A.; Sageman, B.B. Marine black shales: Depositional mechanisms and environments of ancient deposits. *Annu. Rev. Earth Planet. Sci.* **1994**, *22*, 499–551. [[CrossRef](#)]
- Smith, M.G.; Bustin, R.M. Production and preservation of organic matter during deposition of the Bakken formation (Late Devonian and Early Mississippian), Williston Basin. *Palaeogeogr. Palaeoclimatol. Palaeoecol.* **1998**, *142*, 185–200. [[CrossRef](#)]
- Meyers, P.A.; Ishiwatari, R. Lacustrine organic geochemistry—An overview of indicators of organic matter sources and diagenesis in lake sediments. *Org. Geochem.* **1993**, *20*, 867–900. [[CrossRef](#)]
- Liu, C.L.; Li, H.H.; Zhang, X.; Zheng, S.J.; Zhang, L.; Guo, Z.Q.; Liu, J.; Tian, J.X.; Zhang, Y.; Zeng, X. Geochemical characteristics of the Paleogene and Neogene saline lacustrine source rocks in the western Qaidam Basin, northwestern China. *Energy Fuels* **2016**, *30*, 4537–4549. [[CrossRef](#)]
- Zhang, H.F.; Wu, X.S.; Wang, B.; Duan, Y.J.; Qu, Y.; Chen, D.F. Research progress of the enrichment mechanism of sedimentary organics in lacustrine basin. *Acta Seismol. Sin.* **2016**, *34*, 463–477. [[CrossRef](#)]
- Chojnacka, K.; Mikulewicz, M. Biomarkers of trace element status. *Recent Adv. Trace Elem.* **2018**, 457–467.
- Stefanova, M.; Kortenski, J.; Zdravkov, A.; Marinov, S. Paleoenvironmental settings of the Sofia lignite basin: Insights from coal petrography and molecular indicators. *Int. J. Coal Geol.* **2013**, *107*, 45–61. [[CrossRef](#)]
- Summons, R.E.; Metzger, P.; Largeau, C.; Murray, A.P.; Hope, J.M. Polymethylsqualanes from *Botryococcus braunii* in lacustrine sediments and crude oils. *Org. Geochem.* **2002**, *33*, 99–109. [[CrossRef](#)]
- McKirdy, D.M.; Cox, R.E.; Volkman, J.K.; Howell, V.J. Botryococcane in a new class of Australian non-marine crude oils. *Nature* **1986**, *320*, 57–59. [[CrossRef](#)]

20. Chattopadhyay, A.; Dutta, S. Higher plant biomarker signatures of Early Eocene sediments of North Eastern India. *Mar. Pet. Geol.* **2014**, *57*, 51–67. [[CrossRef](#)]
21. Spina, A.; Cirilli, S.; Sorci, A.; Schito, A.; Clayton, G.; Corrado, S.; Rettori, R. Assessing thermal maturity through a multi-proxy approach: A case study from the Permian Faraghan Formation (Zagros Basin, Southwest Iran). *Sediment. Geol.* **2021**, *11*, 484. [[CrossRef](#)]
22. Algeo, T.J.; Maynard, J.B. Trace-element behavior and redox facies in core shales of Upper Pennsylvanian Kansas-type cyclothem. *Chem. Geol.* **2004**, *206*, 289–318. [[CrossRef](#)]
23. Liu, S.M.; Jiang, L.; Liu, B.J.; Zhao, S.H.; Tang, S.H.; Tan, F.R. Investigation of Organic Matter Sources and Depositional Environment Changes for Terrestrial Shale Succession from the Yuka Depression: Implications from Organic Geochemistry and Petrological Analyses. *J. Earth Sci.* **2023**, *34*, 1577–1595. [[CrossRef](#)]
24. Yang, S.Y.; Horsfield, B. Critical review of the uncertainty of Tmax in revealing the thermal maturity of organic matter in sedimentary rocks. *Int. J. Coal Geol.* **2020**, *22*, 357. [[CrossRef](#)]
25. Hartkopf-Fröder, C.; Königshof, P.; Littke, R.; Schwarzbauer, J. Optical thermal maturity parameters and organic geochemical alteration at low grade diagenesis to anchimetamorphism: A review. *Int. J. Coal Geol.* **2015**, *150*, 74–119. [[CrossRef](#)]
26. C Cirilli, S.; Panfili, G.; Buratti, N.; Frixia, A. Paleoenvironmental reconstruction by means of palynofacies and lithofacies analyses: An example from the Upper Triassic subsurface succession of the Hyblean Plateau Petroleum System (SE Sicily, Italy). *Rev. Palaeobot. Palynol.* **2018**, *253*, 70–87. [[CrossRef](#)]
27. Schito, A.; Corrado, S.; Trolese, M.; Aldega, L.; Caricchi, C.; Cirilli, S.; Grigo, D.; Guedes, A.; Romano, C.; Spina, A.; et al. Assessment of thermal evolution of Paleozoic successions of the Holy Cross Mountains (Poland). *Mar. Pet. Geol.* **2017**, *80*, 112–132. [[CrossRef](#)]
28. Schito, A.; Spina, A.; Corrado, S.; Cirilli, S.; Romano, C. Comparing optical and Raman spectroscopic investigations of phytoclasts and sporomorphs for thermal maturity assessment: The case study of Hettangian continental facies in the Holy cross Mts.(central Poland). *Mar. Pet. Geol.* **2019**, *104*, 331–345. [[CrossRef](#)]
29. Chen, Z.H.; Wang, T.-G.; Li, M.J.; Yang, F.L.; Cheng, B. Biomarker geochemistry of crude oils and Lower Paleozoic source rocks in the Tarim Basin, western China: An oil-source rock correlation study. *Mar. Pet. Geol.* **2018**, *96*, 94–112. [[CrossRef](#)]
30. Liu, C.; Chen, S.J.; Su, Z.; Rong, H. Geochemical Characteristics and Origin of Crude Oil and Natural Gas in the Southern Slope Zone, Kuqa Foreland Basin, NW China. *J. Earth Sci.* **2022**, *33*, 820–830. [[CrossRef](#)]
31. Hatch, J.R.; Leventhal, J.S. Relationship between inferred redox potential of the depositional environment and geochemistry of the Upper Pennsylvanian (Missourian) Stark Shale Member of the Dennis Limestone, Wabaunsee County, Kansas, USA. *Chem. Geol.* **1992**, *99*, 65–82. [[CrossRef](#)]
32. Chang, X.; Wang, Y.; Shi, B.; Xu, Y. Charging of Carboniferous volcanic reservoirs in the eastern Chepaizi uplift, junggar basin (northwestern China) constrained by oil geochemistry and fluid inclusion. *AAPG Bull.* **2019**, *103*, 1625–1652. [[CrossRef](#)]
33. Zhang, M.; Zhang, J.; Xu, F.; Li, J.; Liu, J.; Hou, G.; Zhang, P. Paleocene sequence stratigraphy and depositional systems in the Lishui Sag, East China Sea shelf Basin. *Mar. Pet. Geol.* **2015**, *59*, 390–405. [[CrossRef](#)]
34. Su, A.; Chen, H.H.; Cao, L.S.; Lei, M.Z.; Wang, C.W.; Liu, Y.H.; Li, P.J. Genesis, source and charging of oil and gas in Lishui Sag, East China Sea Basin. *Pet. Explor. Dev.* **2014**, *41*, 574–584. [[CrossRef](#)]
35. Guo, Y.H.; Yu, S. Formation of the LS36-1 oil and gas structure in the Lishui Sag, East China Sea Basin. *Pet. Explor. Dev.* **2003**, *30*, 29–31.
36. Jiang, H.Z.; Li, Y.J.; Du, H.L.; Zhang, Y.F. The Cenozoic structural evolution and its influences on gas accumulation in the Lishui Sag, East China Sea Shelf Basin. *J. Nat. Gas Sci. Eng.* **2015**, *22*, 107–118. [[CrossRef](#)]
37. Zhang, Y.Z.; Jiang, Y.M.; Liu, Z.H.; Li, S.; Li, N.; Liu, J.S.; Qiao, P.J.; Zhong, K.; Chen, S.H.; Goh, T.L. Early Cenozoic paleontological assemblages and provenance evolution of the Lishui Sag, East China Sea. *Acta Oceanol. Sin.* **2023**, *42*, 113–122. [[CrossRef](#)]
38. Li, N.; Zhang, J.L.; Shen, W.L.; Liu, Y.; Liu, H.S.; Wang, J.K.; Xie, J. Recovery of the erosion thickness and characterization of the paleogeomorphology in the southern Lishui Sag, East China Sea Shelf basin. *J. Ocean Univ. China* **2020**, *19*, 320–330. [[CrossRef](#)]
39. Fu, C.; Li, S.L.; Li, S.L.; Xu, J.Y.; Huang, Y.Y. Genetic types of mudstone in a closed-lacustrine to open-marine transition and their organic matter accumulation patterns: A case study of the Paleocene source rocks in the East China Sea Basin. *J. Pet. Sci. Eng.* **2022**, *208*, 109343. [[CrossRef](#)]
40. Zhang, L.Y.; Zeng, X.; Zhu, W.L.; Yuan, L.C.; Cai, J.G. Influence of Provenance and the Sedimentary Environment on the Formation of High-Quality Source Rocks in the Paleocene Lishui Sag, China. *ACS Omega* **2022**, *7*, 5791–5803. [[CrossRef](#)]
41. Lei, C.; Yin, S.Y.; Ye, J.; Wu, J.; Wang, Z.; Gao, B. Characteristics and deposition models of the Paleocene source rocks in the Lishui Sag, East China Sea shelf Basin: Evidences from organic and inorganic geochemistry. *J. Pet. Sci. Eng.* **2021**, *200*, 108342. [[CrossRef](#)]
42. Walker, C.T.; Price, N.B. Departure curves for computing paleosalinity from boron in illites and shales. *AAPG Bull.* **1963**, *47*, 833–841. [[CrossRef](#)]
43. Adams, T.D.; Haynes, J.R.; Walker, C.T. Boron in Holocene Illites of the Dovey Estuary, Wales, and its Relationship to Palaeosalinity in CYCLOTHEMS 1. *Sedimentology* **1965**, *4*, 189–195. [[CrossRef](#)]
44. Makeen, Y.M.; Hakimi, M.H.; Abdullah, W.H. The origin, type and preservation of organic matter of the Barremian–Aptian organic-rich shales in the Muglad Basin, Southern Sudan, and their relation to paleoenvironmental and paleoclimate conditions. *Mar. Pet. Geol.* **2015**, *65*, 187–197. [[CrossRef](#)]

45. Li, Y.; Zhang, J.L.; Liu, Y.; Shen, W.L.; Chang, X.C.; Sun, Z.Q.; Xu, G.C. Organic geochemistry, distribution and hydrocarbon potential of source rocks in the Paleocene, Lishui Sag, East China Sea Shelf Basin. *Mar. Pet. Geol.* **2019**, *107*, 382–396. [[CrossRef](#)]
46. Zhu, W.L.; Zhong, Z.; Fu, X.W.; Chen, C.F.; Zhang, M.Q.; Gao, S.L. The formation and evolution of the East China Sea Shelf Basin: A new view. *Earth Sci. Rev.* **2019**, *190*, 89–111. [[CrossRef](#)]
47. Tian, B.; Zhao, J.M.; Zheng, Y.W. The hydrocarbon generation controlled by source rocks and heat in the offshore superimpose rift-subsidence basin: A case study from Lishui-jiaojiang Sag. *J. Inner Mongolia Univ. Sci. Technol.* **2021**, *40*, 137–143. [[CrossRef](#)]
48. Xu, B.; Hu, B.Y.; Zhang, Y.N.; Gu, Z.P.; Hong, Q. Geochemical Characteristics of Light Hydrocarbons in Crude Oil from Lishui 36-1 Oil and Gas Field. *J. Chongqing Univ. Sci. Technol. (Nat. Sci. Ed.)* **2020**, *22*, 12–18. [[CrossRef](#)]
49. Zhong, K.; Zhu, W.L.; Gao, S.L.; Fu, X.W. Key Geological Questions of the Formation and Evolution and Hydrocarbon Accumulation of the East China Sea Shelf Basin. *Earth Sci.* **2018**, *43*, 3485–3497. [[CrossRef](#)]
50. Miller, K.G.; Kominz, M.A.; Browning, J.V.; Wright, J.D.; Mountain, G.S.; Katz, M.E.; Pekar, S. The Phanerozoic record of global sea-level change. *Science* **2005**, *31*, 1293–1298. [[CrossRef](#)]
51. Zhang, C.Y.; Guan, S.W.; Wu, L.; Ren, R.; Xiong, L.Q. Geochemical characteristics and its paleo-environmental significance of the Lower Cambrian carbonate in the northwestern Tarim Basin: A case study of Well Shutan-1. *Bull. Geol. Sci. Technol.* **2021**, *40*, 99–111. [[CrossRef](#)]
52. McLennan, S.M. Rare earth elements in sedimentary rocks; influence of provenance and sedimentary processes. *Rev. Mineral Geochem.* **1989**, *21*, 169–200.
53. Hunt, J. *Petroleum Geochemistry and Geology*; Freeman Company: New York, NY, USA, 1996; 743p.
54. Zachos, J.; Pagani, M.; Sloan, L.; Thomas, E.; Billups, K. Trends, Rhythms, and Aberrations in Global Climate 65 Ma to Present. *Science* **2001**, *292*, 686–693. [[CrossRef](#)] [[PubMed](#)]
55. Sun, Z.Q.; Zhang, J.L.; Liu, Y.; Shen, W.L.; Li, Y.; Li, L.J. Sedimentological signatures and identification of Paleocene sedimentary facies in the Lishui sag, East China Sea Shelf basin. *Can. J. Earth Sci.* **2020**, *57*, 377–395. [[CrossRef](#)]
56. Volkman, J.K. A review of sterol markers for marine and terrigenous organic matter. *Org. Geochem.* **1986**, *9*, 83–99. [[CrossRef](#)]
57. You, H.T.; Cheng, R.H.; Liu, C.L. Review of Paleosalinity Recovering Methods. *World Geol.* **2002**, *21*, 111–117.
58. Wei, W.; Algeo, T.J. Elemental proxies for paleosalinity analysis of ancient shales and mudrocks. *Geochim. Cosmochim. Acta* **2020**, *287*, 341–366. [[CrossRef](#)]
59. Wang, S.L.; Ren, L.y.; Wang, Y.; Li, J.D.; He, F.; Wang, Y.X. Characteristic of diagenesis saline lake environment and its effect on high-porosity zones. *Pet. Explor. Dev.* **2003**, *30*, 47–49.
60. Yang, H.; Liu, C.L.; Wang, F.L.; Tang, G.M.; Li, G.X.; Zeng, X.X.; Wu, Y.P. Geochemical characteristics and environmental implications of source rocks of the Dongying Formation in southwest subsag of Bozhong Sag. *Bull. Geol. Sci. Technol.* **2023**, *42*, 339–349. [[CrossRef](#)]
61. Sepúlveda, J.; Wendler, J.; Leider, A.; Kuss, H.J.; Hinrichs, K.U. Molecular isotopic evidence of environmental and ecological changes across the Cenomanian–Turonian boundary in the Levant platform of central Jordan. *Org. Geochem.* **2009**, *40*, 553–568. [[CrossRef](#)]
62. Zhu, Y.M.; Weng, H.X.; Su, A.G.; Liang, D.G.; Peng, D.H. Geochemical characteristics of Tertiary saline lacustrine oils in the Western Qaidam Basin, northwest China. *Appl. Geochem.* **2005**, *20*, 1875–1889. [[CrossRef](#)]
63. Guan, Y.Z. The element, clay mineral, and depositional environment in Herein Sand Land. *J. Desert Res.* **1992**, *12*, 9–15.
64. Tang, L.; Song, Y.; Pang, X.Q.; Jiang, Z.X.; Guo, Y.C.; Zhang, H.G.; Pan, Z.H.; Jiang, H. Effects of paleo sedimentary environment in saline lacustrine basin on organic matter accumulation and preservation: A case study from the Dongpu Depression, Bohai Bay Basin, China. *J. Pet. Sci. Eng.* **2020**, *185*, 106669. [[CrossRef](#)]
65. Cao, J.; Wu, M.; Chen, Y.; Hu, K.; Bian, L.Z.; Wang, L.G.; Zhang, Y. Trace and rare earth element geochemistry of Jurassic mudstones in the northern Qaidam basin, northwest China. *Geochemistry* **2012**, *72*, 245–252. [[CrossRef](#)]
66. Hakimi, M.H.; Abdullah, W.H.; Makeen, Y.M.; Saeed, S.A.; Al-Hakame, H.; Al-Moliki, T.; Al-Sharabi, K.Q.; Hatem, B.A. Geochemical characterization of the Jurassic Amran deposits from Sharab area (SW Yemen): Origin of organic matter, paleoenvironmental and paleoclimate conditions during deposition. *J. Afr. Earth Sci.* **2017**, *129*, 579–595. [[CrossRef](#)]
67. Khan, D.; Liang, C.; Qiu, L.; Kamran, M.I.R.Z.A.; Wang, Y.; Kashif, M.; Teng, J. Depositional Environment and Lithofacies Analyses of Eocene Lacustrine Shale in the Bohai Bay Basin: Insights from Mineralogy and Elemental Geochemistry. *Acta Geol. Sin.* **2023**, *9*, 589–609. [[CrossRef](#)]
68. Liu, J.H.; Wu, Z.X.; Yu, S.; Jia, D.H. Paleocene trace element geochemistry and its geological significance in Lishui sag. *China Offshore Oil and Gas* **2005**, *17*, 8–11.
69. Liu, E.T.; Chen, S.; Yan, D.T.; Deng, Y.; Wang, H.; Jing, Z.H.; Pan, S.Q. Detrital zircon geochronology and heavy mineral composition constraints on provenance evolution in the western Pearl River Mouth basin, northern south China sea: A source to sink approach. *Mar. Petrol. Geol.* **2022**, *145*, 105884. [[CrossRef](#)]
70. Liu, E.T.; Wang, H.; Feng, Y.X.; Pan, S.Q.; Jing, Z.H.; Ma, Q.L.; Gan, H.J.; Zhao, J.X. Sedimentary architecture and provenance analysis of a sublacustrine fan system in a half-graben rift depression of the South China Sea. *Sediment. Geol.* **2020**, *409*, 105781. [[CrossRef](#)]
71. Smith, M.E.; Carroll, A.R. *Introduction to the Green River Formation. Stratigraphy and Paleolimnology of the Green River Formation, Western USA*; Springer: Cham, Switzerland, 2015; pp. 1–12.

72. Graf, J.W.; Carroll, A.R.; Smith, M.E. *Lacustrine Sedimentology, Stratigraphy and Stable Isotope Geochemistry of the Tipton Member of the Green River Formation. Stratigraphy and Paleolimnology of the Green River Formation, Western USA*; Springer: Cham, Switzerland, 2015; pp. 31–60.
73. Bakun, A. Global climate change and intensification of coastal ocean upwelling. *Science* **1990**, *247*, 198–201. [[CrossRef](#)] [[PubMed](#)]
74. Broecker, W.S. Abrupt climate change: Causal constraints provided by the paleoclimate record. *Earth-Sci. Rev.* **2000**, *51*, 137–154. [[CrossRef](#)]
75. Sorci, A.; Cirilli, S.; Spina, A.; Ghorbani, M.; Rettori, R. Facies analysis and depositional environment of a late Cambrian mixed carbonate-siliciclastic ramp from the Zard Kuh Mountain (Zagros Basin, south-western Iran). *Sediment. Geol.* **2023**, *449*, 106370. [[CrossRef](#)]
76. Feldman, H.R.; Franseen, E.K.; Joeckel, R.M.; Heckel, P.H. Impact of longer-term modest climate shifts on architecture of high-frequency sequences (cyclothems), Pennsylvanian of Midcontinent USA. *J. Sediment. Res.* **2005**, *75*, 350–368. [[CrossRef](#)]
77. Wang, Q.F.; Jiang, F.J.; Ji, H.C.; Jiang, S.; Liu, X.H.; Zhao, Z.; Wu, Y.Q.; Xiong, H.; Li, Y.; Wang, Z. Effects of paleosedimentary environment on organic matter enrichment in a saline lacustrine rift basin-A case study of Paleogene source rock in the Dongpu Depression, Bohai Bay Basin. *J. Pet. Sci. Eng.* **2020**, *195*, 107658. [[CrossRef](#)]
78. Quan, Y.B.; Hao, F.; Liu, J.Z.; Zhao, D.J.; Tian, J.Q.; Wang, Z.F. Source rock deposition controlled by tectonic subsidence and climate in the western Pearl River Mouth Basin, China: Evidence from organic and inorganic geochemistry. *Mar. Pet. Geol.* **2017**, *79*, 1–17. [[CrossRef](#)]
79. Gautier, D.L. Cretaceous shales from the western interior of North America: Sulfur/carbon ratios and sulfur-isotope composition. *Geology* **1986**, *14*, 225–228. [[CrossRef](#)]
80. Curtis, J.B. Fractured shale-gas systems. *AAPG Bull.* **2002**, *86*, 1921–1938. [[CrossRef](#)]
81. Ren, J.Y.; Tamaki, K.; Li, S.T.; Junxia, Z. Late Mesozoic and Cenozoic rifting and its dynamic setting in Eastern China and adjacent areas. *Tectonophysics* **2002**, *344*, 175–205. [[CrossRef](#)]
82. Tian, Y.; Ye, J.R.; Lei, C.; Yang, B.L.; Dan, C.; He, Q.Y.; Liu, Y.M. Development controlling factors and forming model for source rock of Yueguifeng Formation in Lishui-jiaojiang sag, the East China Sea Continental Shelf Basin. *Earth Sci.* **2016**, *41*, 1561–1571. [[CrossRef](#)]
83. Raymo, M.E.; Ruddiman, W.F.; Froelich, P.N. Influence of late Cenozoic mountain building on ocean geochemical cycles. *Geology* **1988**, *16*, 649–653. [[CrossRef](#)]
84. Jørgensen, B.B.; Isaksen, M.F.; Jannasch, H.W. Bacterial sulfate reduction above 100 C in deep-sea hydrothermal vent sediments. *Science* **1992**, *258*, 1756–1757. [[CrossRef](#)]
85. Gonçalves, F.T. Organic and isotope geochemistry of the Early Cretaceous rift sequence in the Camamu Basin, Brazil: Paleolimnological inferences and source rock models. *Org. Geochem.* **2002**, *33*, 67–80. [[CrossRef](#)]
86. Bohacs, K.M.; Carroll, A.R.; Neal, J.E.; Mankiewicz, P.J. *Lake-Basin Type, Source Potential, and Hydrocarbon Character: An Integrated Sequence-Stratigraphic-Geochemical Framework*; Studies in Geology #46; American Association of Petroleum Geologists: Tulsa, OK, USA, 2000; pp. 3–33.
87. Tissot, B.P. Recent advances in petroleum geochemistry applied to hydrocarbon exploration. *AAPG Bull.* **1984**, *68*, 546–563. [[CrossRef](#)]
88. Dembicki, H., Jr. Three common source rock evaluation errors made by geologists during prospect or play appraisals. *AAPG Bull.* **2009**, *93*, 341–356. [[CrossRef](#)]
89. Chen, J.P.; Ge, H.P.; Chen, X.D.; Deng, C.P.; Liang, D.G. Classification and origin of natural gases from Lishui Sag, the East China Sea Basin. *Sci. China, Ser. D Earth Sci.* **2008**, *51*, 122–130. [[CrossRef](#)]
90. Lei, C.; Yin, S.Y.; Ye, J.R.; Wu, J.F. Geochemical characteristics and hydrocarbon generation history of the Paleogene source rocks in the Jiaojiang Sag, East China Sea Basin. *J. Earth Sci.* **2021**, *46*, 3575–3587. [[CrossRef](#)]

**Disclaimer/Publisher’s Note:** The statements, opinions and data contained in all publications are solely those of the individual author(s) and contributor(s) and not of MDPI and/or the editor(s). MDPI and/or the editor(s) disclaim responsibility for any injury to people or property resulting from any ideas, methods, instructions or products referred to in the content.